SHOCK AND VIBRATION STRESS AS A FUNCTION OF VELOCITY
Revision G

By Tom Irvine
Email: tom@vibrationdata.com

April 11, 2013

Variables

$\hat{c}$	=	Distance to neutral axis	I	=	Area moment of inertia
c	=	Wave speed in the material	K	=	Shear factor
h	=	thickness	L	=	Length
k	=	Spring stiffness or wave number depending on context	M	=	Bending moment
u	=	Displacement	U	=	Total energy
v	=	Velocity	V	=	Shear force
x	=	Longitudinal Displacement	$\ddot{W}$	=	Base acceleration
z	=	Transverse Displacement	σ	=	Normal stress
A	=	Cross section area	τ	=	Shear stress
$\hat{C}$	=	Constant of proportionality	ρ	=	Mass per volume
D	=	Plate stiffness factor	$\hat{\rho}$	=	Mass per length
E	=	Elastic modulus	ϕ	=	Phase angle
G	=	Shear modulus	ω_n	=	Natural frequency (rad/sec)

Note that the characteristic impedance is ρc.

Introduction

Shock and vibration environments produce dynamic stresses which can cause material failure in structures. The potential failure modes include fatigue, yielding, and ultimate stress limit.

F.V. Hunt wrote a seminal paper on this subject, titled "Stress and Stress Limits on the Attainable Velocity in Mechanical Vibration," published in 1960 in Reference 1. This paper gave the relationship between stress and velocity for a number of sample structures.

H. Gaberson continued research on stress and modal velocity with a series of papers and presentations, as shown in References 2 through 4.

The purpose of this paper is to explore the work of Hunt, Gaberson, and others. Derivations are given relating stress and velocity for a number of structures. Some of these examples overlap the work of previous sources. Other examples are original. In addition, this paper presents some unique data samples for shock events, with the corresponding spectra plotted in tripartite format.

Stress in an Infinite Rod in Longitudinal Free Vibration

Consider an infinitely long longitudinal rod undergoing a traveling wave response. The stress is proportional to the velocity as follows.

$$\sigma(x,t) = -\rho c \; v(x,t) \tag{1}$$

This equation is given in References 1 through 6.

A derivation is given in Appendix A.

Stress in a Finite, Fixed-Free Rod, in Longitudinal Free Vibration

Consider a fixed-free rod subjected to initial velocity excitation.

The modal stress is proportional to the modal velocity as follows.

$$[\sigma_n]_{max} = \rho c \; v_{n,max} = \rho c \; \omega_n \; \hat{u}_{n,max} \tag{2}$$

A derivation is given in Appendix B.

Gaberson showed that this same equation applies to other boundaries conditions of finite rod in Reference 2.

Stress in a Finite, Fixed-Free Rod, Longitudinal Response Excited by Resonant Base Excitation

Consider a fixed-free rod subjected to base excitation. Equation (2) applies as long as the excitation is sinusoidal with a frequency equal to the natural frequency of the corresponding mode. The derivation is given in Appendix C.

Stress in a Shear Beam in Free Vibration

Consider the free vibration of a shear beam with a rectangular cross-section.

The modal shear stress is proportional to the modal velocity as follows, from the derivation in Appendix D.

$$\tau_{n,max} = 1.5 \frac{\rho c}{K} v_{n,max} \tag{3}$$

Stress due to Bending in a Bernoulli-Euler Beam in Free Vibration

Consider the bending vibration of a simply-supported beam. The modal stress due to bending is proportional to the modal velocity as follows, from the derivation in Appendix E.

$$\sigma_{max} = E \hat{c} \left[\frac{\partial^2}{\partial x^2} y_n(x,t) \right]_{max} = \hat{c} \sqrt{\frac{E A \rho}{I}} \; v_{n,max} \tag{4}$$

Note this equation applies to other boundary condition cases per Reference 1.

Equation (4) can be simplified as follows:

$$\sigma_{max} = \hat{k} \, \rho c \, v_{n,max} \tag{5}$$

Values for the $\hat{k}$ constant for typical cross-sections are:

Cross-section	$\hat{k}$
Solid Circular	2
Rectangular	$\sqrt{3}$

Stress due to Bending in a Bernoulli-Euler Beam Excited by Resonant Base Excitation

Consider the bending vibration of a simply-supported beam subjected to resonant base excitation. The modal stress due to bending is proportional to the modal velocity as shown in the derivation in Appendix F. The resulting stress-velocity equation is the same as equations (4) and (5).

Stress due to Bending in a Plate in Free Vibration

Consider bending in a rectangular plate with all edges simply-supported. The following intermodal stress equations are derived in Appendix G.

$$\left[\sigma_{int,x}\right]_{max} = \rho c \sqrt{\frac{3}{1-\nu^2}} \left[\frac{L_y{}^2 + \nu L_x{}^2}{L_y{}^2 + L_x{}^2}\right] v_{int,max} \tag{6}$$

$$\left[\sigma_{int,y}\right]_{max} = \rho c \sqrt{\frac{3}{1-\nu^2}} \left[\frac{L_x{}^2 + \nu L_y{}^2}{L_y{}^2 + L_x{}^2}\right] v_{int,max} \tag{7}$$

Complex Equipment

Bateman wrote in Reference 7:

> Of the three motion parameters (displacement, velocity, and acceleration) describing a shock spectrum, velocity is the parameter of greatest interest from the viewpoint of damage potential. This is because the maximum stresses in a structure subjected to a dynamic load typically are due to the responses of the normal modes of the structure, that is, the responses at natural frequencies. At any given natural frequency, stress is proportional to the modal (relative) response velocity.

Bateman then gave a formula equivalent to the following equation for mode n.

$$\left[\sigma_n\right]_{max} = \hat{C}\,\sqrt{E\rho}\,\left[V_n\right]_{max} \tag{8}$$

where

$\hat{C}$ is a constant of proportionality dependent upon the geometry of the structure, often assumed for complex equipment to be $4 < \hat{C} < 8$.

Sweitzer, Hull & Piersol also gave equation (8) in Reference 28, with the same constant of proportionality limits for complex equipment. They also noted that $\hat{C} \approx 2$ for all normal modes of homogeneous plates and beams.

Spring-Mass System Example, Free Vibration

Consider the system shown in Figure 1.

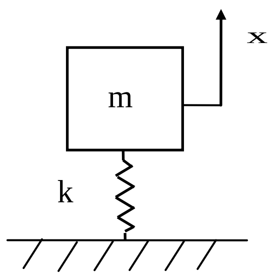

Figure 1.

The energy equation is

$$U = \frac{1}{2} m [v_{max}]^2 = \frac{1}{2} k [x_{max}]^2 \tag{9}$$

The velocity is thus square root of twice the peak energy per unit mass that is stored in the oscillator. The relationship does not directly depend on the natural frequency.

$$v_{max} = \sqrt{\frac{2U}{m}} \tag{10}$$

Examples

Numerical examples using the formulas derived in this paper are given in Reference 27.

Conclusion

Stress-Velocity Relationship

Modal stress is directly proportional to modal velocity for both free vibration and resonant excitation. The proportionality equation does not depend on frequency, although the velocity itself depends on frequency.

There are limitations to any stress-velocity equation, however. Crandall noted in Reference 26 that stress and velocity may each have concentrations, particularly for nonuniform structures.

Shock Response Spectra Dynamic Range

Six shock pulses were considered in terms of their respective shock response spectra. One was an analytical half-sine shock pulse. Another was an earthquake strong-motion time history. The other four were measured shock events from rocket vehicles or motors. The dynamic range for the velocity ranged from 12 to 33 dB among these six samples. In each case the amplitude range for velocity was less than or equal to that for the corresponding displacement and acceleration.

Thus, the response velocity is frequency-dependent, although less so than either displacement or acceleration.

The natural frequency of any component attached to the base structure must still be considered with respect to the velocity spectrum.

Shock response spectra should be plotted in tripartite format so that the effect of displacement, velocity and acceleration can be considered together on a single plot. This plot may be in addition to separate plots of each of the three amplitude metrics.

Again, modal stress is directly proportional to modal velocity. But other failure modes may have better correlation with either displacement or acceleration. Loss of sway space must be considered with respect to relative displacement, for example. Thus attention should be given to each of the three amplitude metrics.

References

1. F.V. Hunt, Stress and Strain Limits on the Attainable Velocity in Mechanical Systems, JASA, 32(9) 1123-1128, 1960.

2. Gaberson and Chalmers, Modal Velocity as a Criterion of Shock Severity, Shock and Vibration Bulletin, Naval Research Lab, December 1969.

3. H. Gaberson, Using the Velocity Shock Spectrum for Damage Potential, SAVIAC, 74th Symposium, San Diego, CA, 2003.

4. H. Gaberson, An Overview of the Use of the Pseudo Velocity Shock Spectrum, Space Craft and Launch Vehicle, Dynamic Environments Workshop, The Aerospace Corporation, El Segundo, CA, 2007.

5. K. Graff, Wave Motions in Elastic Solids, Dover, New York, 1991.

6. R. Clough and J. Penzien, Dynamics of Structures, McGraw-Hill, New York, 1975.

7. A. Piersol and T. Paez, eds., Harris' Shock and Vibration Handbook, 6th Edition, NY, McGraw-Hill, 2010.

8. T. Irvine, Notes on Mechanical Shock and Vibration Waves, Revision B, Vibrationdata, 2000.

9. T. Irvine, Initial Velocity Excitation of the Longitudinal Modes in a Beam for Pyrotechnic Shock Simulation, Vibrationdata, 2008.

10. T. Irvine, Rod Response to Longitudinal Base Excitation, Steady-State and Transient, Rev B, Vibrationdata, 2009.

11. T. Irvine, Natural Frequencies of a Shear Beam, Vibrationdata, 2009.

12. W. Thomson, Theory of Vibration with Applications, Second Edition, Prentice-Hall, New Jersey, 1981.

13. T. Irvine, Bending Frequencies of Beams, Rods, and Pipes, Rev M, Vibrationdata, 2010.

14. T. Irvine, Natural Frequencies of Rectangular Plate Bending Modes, Vibrationdata, 2008.

15. T. Irvine, An Introduction to the Shock Response Spectrum Rev P, Vibrationdata, 2002.

16. T. Irvine, The Pseudo Velocity Shock Response Spectrum, Revision A, Vibrationdata, 2010.

17. T. Irvine, Steady-State Vibration Response of a Simply-Supported Beam Subjected to Base Excitation, Vibrationdata, 2010.

18. MIL-STD-810E, Environmental Test Methods and Engineering Guidelines, U.S. Department of Defense, 1989.

19. MIL-STD-810F, Environmental Test Methods and Engineering Guidelines, U.S. Department of Defense, 2000.

20. MIL-STD-810G, Environmental Test Methods and Engineering Guidelines, U.S. Department of Defense, 2008.

21. C. Harris and C. E. Crede, eds., Shock and Vibration Handbook, 5th Edition, McGraw-Hill, New York, 2001. See Bateman, Shock Testing Machines, Chapter 27.

22. T. Irvine, Building Vibration Standards, Revision A, Vibrationdata, 2001.

23. G. Bonde, et al, Criteria for Acceptable Traffic-Induced Vibrations, Institute of Technology, Uppsala University, UPTEC 81 42 R, TRAVI-K, 1981.

24. H. Bachmann, et al., Vibration Problems in Structures, Birkhauser Verlag, Berlin, 1995.

25. C. Gordon, Generic Vibration Criteria for Vibration-Sensitive Equipment, SPIE Proceedings Volume 1619, 1991.

26. S. Crandall, Relation between Stress and Velocity in Resonant Vibration, Acoustical Society of American, December 1962.

27. T. Irvine, Notes on Internal and Transmitted Forces in Vibrating Multi-degree-of-freedom Systems, Vibrationdata, 2010.

28. A. Piersol & T. Paez, Harris' Shock and Vibration Handbook, Sixth Edition, McGraw-Hill, New York, 2010. See Sweitzer, Hull & Piersol; Chapter 40, Equipment Design.

29. H. Gaberson, Shock Severity Estimation, Sound & Vibration, January 2012.

30. Morse, R., presentation at Spacecraft & Launch Vehicle Dynamics Environments Workshop Program, Aerospace Corp., El Segundo, CA, June 20, 2000.

Table 2. Appendix Organization

Appendix	Topic
A	Stress in an Infinite Rod in Longitudinal Free Vibration
B	Stress in a Finite, Fixed-Free Rod, in Longitudinal Free Vibration
C	Stress in a Finite, Fixed-Free Rod, Longitudinal Response Excited by Resonant Base Excitation
D	Stress in a Shear Beam in Free Vibration
E	Stress due to Bending in a Bernoulli-Euler Beam in Free Vibration
F	Stress due to Bending in a Bernoulli-Euler Beam Excited by Base Excitation
G	Stress in a Rectangular Plate in Free Vibration
H	MIL-STD-810E & Morse Chart
I	MIL-STD-810G
J	Pseudo Velocity Shock Response Spectrum
K	Half-Sine Pulse
L	El Centro Earthquake
M	Re-entry Vehicle Separation Shock
N	SR-19 Motor Ignition
O	Space Shuttle Solid Rocket Booster Water Impact
P	V-band/Bolt-Cutter Shock
Q	Maximum Velocity Summary
R	Velocity Limits of Materials

Table 2. Appendix Organization (Continued)	
Appendix	Topic
S	Characteristic Impedance Values
T	Velocity Limits for Buildings
U	Velocity Limits for Vibration Sensitive Equipment

APPENDIX A

Stress in an Infinite Rod in Longitudinal Free Vibration

The following derivation is based on Reference 8.

Consider the free longitudinal vibration in a rod. The governing equation is

$$\frac{\partial^2 u}{\partial x^2} = \left(\frac{1}{c^2}\right)\frac{\partial^2 u}{\partial t^2} \tag{A-1}$$

Now consider that the rod has an infinite length.

A proposed traveling wave solution to equation (A-1) is

$$u(x,t) = A\sin(kx - \omega t - \phi) \tag{A-2}$$

Taking derivatives of the proposed traveling-wave solution

$$\frac{\partial u}{\partial x} = kA\cos(kx - \omega t - \phi) \tag{A-3}$$

$$\frac{\partial^2 u}{\partial x^2} = -k^2 A\sin(kx - \omega t - \phi) \tag{A-4}$$

$$\frac{\partial u}{\partial t} = -\omega A\cos(kx - \omega t - \phi) \tag{A-5}$$

$$\frac{\partial^2 u}{\partial t^2} = -\omega^2 A\sin(kx - \omega t - \phi) \tag{A-6}$$

By substitution,

$$-Ak^2 \sin(kx - \omega t - \phi) = \left[\frac{1}{c^2}\right]\left[-\omega^2 A\sin(kx - \omega t - \phi)\right] \tag{A-7}$$

The following constraint results from the substitution

$$k^2 = \frac{\omega^2}{c^2} \tag{A-8}$$

The wavenumber is thus

$$k = \frac{\omega}{c} \tag{A-9}$$

Thus,

$$u(x,t) = A \sin\left[\omega\left(\frac{x}{c} - t\right) - \phi\right] \tag{A-10}$$

$$\frac{\partial}{\partial x} u(x,t) = \frac{\omega}{c} A \cos\left[\omega\left(\frac{x}{c} - t\right) - \phi\right] \tag{A-11}$$

$$\frac{\partial}{\partial t} u(x,t) = -\omega A \cos\left[\omega\left(\frac{x}{c} - t\right) - \phi\right] \tag{A-12}$$

$$\frac{\partial}{\partial x} u(x,t) = -\frac{1}{c}\frac{\partial}{\partial t} u(x,t) \tag{A-13}$$

The axial stress $\sigma(x,t)$ is

$$\sigma(x,t) = E\frac{\partial}{\partial x} u(x,t) = -\frac{1}{c}\frac{\partial}{\partial t} u(x,t) = \frac{\omega E}{c} A \cos\left[\omega\left(\frac{x}{c} - t\right) - \phi\right] \tag{A-14}$$

Define the velocity as $v(x,t)$.

$$v(x,t) = \frac{\partial}{\partial t} u(x,t) \tag{A-15}$$

The axial stress can thus be calculated from the velocity

$$\sigma(x,t) = -\frac{E}{c}\, v(x,t) \tag{A-16}$$

Or equivalently,

$$\sigma(x,t) = -\rho c \; v(x,t) \qquad \text{(A-17)}$$

where ρc is the characteristic specific impedance of the rod material.

APPENDIX B

Stress in a Finite, Fixed-Free Rod, in Longitudinal Free Vibration

The following derivation is taken from Reference 9.

Consider a long, slender, free-free rod that is dropped such that it has a uniform initial velocity of V as it strikes the ground. Further assume that the rod becomes attached to the ground at impact such that its boundary conditions become fixed-free.

The displacement is

$$u(x,t) = \frac{8\,v\,L}{\pi^2\,c} \sum_{n=1,3,5,\ldots}^{\infty} \left\{ \frac{1}{n^2} \sin\left(\frac{n\,\pi\,x}{2L}\right) \sin(\omega_n\,t) \right\} \tag{B-1}$$

$$\frac{\partial}{\partial x} u(x,t) = \frac{8\,v\,L}{\pi^2\,c} \left(\frac{\pi}{2L}\right) \sum_{n=1,3,5,\ldots}^{\infty} \left\{ \frac{1}{n} \cos\left(\frac{n\,\pi\,x}{2L}\right) \sin(\omega_n\,t) \right\} \tag{B-2}$$

$$\frac{\partial}{\partial x} u(x,t) = \frac{4\,v}{\pi\,c} \sum_{n=1,3,5,\ldots}^{\infty} \left\{ \frac{1}{n} \cos\left(\frac{n\,\pi\,x}{2L}\right) \sin(\omega_n\,t) \right\} \tag{B-3}$$

where

$$\omega_n = \frac{n\,\pi\,c}{2L} \tag{B-4}$$

$$\frac{\partial}{\partial t} u(x,t) = \frac{8\,v\,L}{\pi^2\,c} \left(\frac{\pi\,c}{2L}\right) \sum_{n=1,3,5,\ldots}^{\infty} \left\{ \frac{1}{n} \sin\left(\frac{n\,\pi\,x}{2L}\right) \cos(\omega_n\,t) \right\} \tag{B-5}$$

$$\frac{\partial}{\partial t} u(x,t) = \frac{4\,v}{\pi} \sum_{n=1,3,5,\ldots}^{\infty} \left\{ \frac{1}{n} \sin\left(\frac{n\,\pi\,x}{2L}\right) \cos(\omega_n\,t) \right\} \tag{B-6}$$

Now let

$$u(x,t) = \left(\frac{8\,v\,L}{\pi^2\,c}\right) \sum_{n=1,3,5,\ldots}^{\infty} \hat{u}_n\,(x,t) \tag{B-7}$$

The modal displacement is

$$\hat{u}_n\,(x,t) = \frac{1}{n^2} \sin\left(\frac{n\,\pi\,x}{2L}\right) \sin(\omega_n\,t) \tag{B-8}$$

$$\frac{\partial}{\partial x}\,\hat{u}_n\,(x,t) = \frac{\pi}{2n\,L} \cos\left(\frac{n\,\pi\,x}{2L}\right) \sin(\omega_n\,t) \tag{B-9}$$

$$\frac{\partial}{\partial t}\,\hat{u}_n\,(x,t) = \left(\frac{\pi\,c}{2\,n\,L}\right) \sin\left(\frac{n\,\pi\,x}{2L}\right) \cos(\omega_n\,t) \tag{B-10}$$

$$\left[\frac{\partial\,\hat{u}_n}{\partial x}\right]_{max} = \left[\frac{\partial\,\hat{u}_n}{\partial t}\right]_{max} \tag{B-11}$$

The maximum stress per mode n is thus proportional to the maximum modal velocity.

Note that the maximum stress location will vary from that of the maximum velocity.

The peak values of harmonic displacement, velocity and acceleration have their maxima at the antinodes of motion, whereas the peak values of stress and strain have their maxima at the nodes, per Reference 1. This statement applies to a finite rod undergoing standing wave oscillations.

$$[\sigma_n]_{max} = \frac{E}{c}\left[\frac{\partial\,\hat{u}_n}{\partial t}\right]_{max} = \left(\frac{E}{c}\right)\left(\frac{8\,v\,L}{\pi^2\,c}\right)\left(\frac{\pi\,c}{2\,n\,L}\right) \tag{B-12}$$

$$[\sigma_n]_{max} = \frac{E}{c}\left[\frac{\partial\,\hat{u}_n}{\partial t}\right]_{max} = \left(\frac{4\,v\,E}{n\,\pi\,c}\right) \tag{B-13}$$

Note

$$\left[\frac{\partial \hat{u}_n}{\partial t}\right]_{max} = \omega_n \left[\hat{u}_n\right]_{max} \tag{B-14}$$

The maximum stress is thus

$$\left[\sigma_n\right]_{max} = \frac{E}{c}\left[\frac{\partial \hat{u}_n}{\partial t}\right]_{max} = \frac{E}{c}\,\omega_n \left[\hat{u}_n\right]_{max} \tag{B-15}$$

Or in terms of the characteristic impedance,

$$\left[\sigma_n\right]_{max} = \rho c\left[\frac{\partial \hat{u}_n}{\partial t}\right]_{max} = \rho c\ \omega_n \left[\hat{u}_n\right]_{max} \tag{B-16}$$

The advantage of calculating stress from velocity is that the natural frequency term is not required, as it is for calculating stress from displacement.

Furthermore the characteristic impedance ρc plays the role of a *transfer impedance* which expresses the ratio of the stress at a node of motion to the velocity at an associated antinode, per Reference 1. Again, this applies to a finite rod undergoing standing wave oscillations.

APPENDIX C

Stress in a Finite, Fixed-Free Rod, Longitudinal Response Excited by Resonant Base Excitation

The following derivation is taken from Reference 10.

$$U(x,\omega) = \ddot{W}(\omega)\sum_{n=1}^{p}\left[\frac{-\Gamma_n \hat{U}_n(x)}{(\omega_n{}^2 - \omega^2) + j(2\xi\omega\omega_n)}\right] \tag{C-1}$$

The mode shape is

$$\hat{U}_n(x) = \sqrt{\frac{2}{mL}}\sin\left(\frac{\omega_n x}{c}\right) \tag{C-2}$$

$$\frac{d}{dx}\hat{U}_n(x) = \frac{\omega_n}{c}\sqrt{\frac{2}{mL}}\cos\left(\frac{\omega_n x}{c}\right) \tag{C-3}$$

The strain is

$$\frac{\partial}{\partial x}U(x,\omega) = \ddot{W}(\omega)\sum_{n=1}^{p}\left[\frac{-\Gamma_n \frac{d}{dx}\hat{U}_n(x)}{(\omega_n{}^2 - \omega^2) + j(2\xi\omega\omega_n)}\right] \tag{C-4}$$

$$\frac{\partial}{\partial x}U(x,\omega) = \ddot{W}(\omega)\,\frac{1}{c}\sqrt{\frac{2}{mL}}\,\sum_{n=1}^{p}\left[\frac{-\Gamma_n\,\omega_n\,\cos\left(\frac{\omega_n x}{c}\right)}{(\omega_n{}^2 - \omega^2) + j(2\xi\omega\omega_n)}\right] \tag{C-5}$$

On a modal basis,

$$\left[\frac{\partial}{\partial x} U_n(x,\omega)\right]_{max} = \ddot{W}(\omega)\,\frac{1}{c}\sqrt{\frac{2}{mL}}\left[\frac{-\Gamma_n\,\omega_n}{(\omega_n{}^2-\omega^2)+j\left(2\xi\,\omega\omega_n\right)}\right]_{max} \qquad \text{(C-6)}$$

The phase can be ignored.

$$\left[\frac{\partial}{\partial x} U_n(x,\omega)\right]_{max} = \ddot{W}(\omega)\,\frac{1}{c}\sqrt{\frac{2}{mL}}\left[\frac{-\Gamma_n\,\omega_n}{\sqrt{(\omega_n{}^2-\omega^2)^2+\left(2\xi\,\omega\omega_n\right)^2}}\right] \qquad \text{(C-7)}$$

The velocity v in the frequency domain is

$$v(x,\omega) = j\omega\,\ddot{W}(\omega)\sum_{n=1}^{p}\left[\frac{-\Gamma_n\,\hat{U}_n(x)}{(\omega_n{}^2-\omega^2)+j\left(2\xi\,\omega\omega_n\right)}\right] \qquad \text{(C-8)}$$

$$\hat{U}_n(x) = \sqrt{\frac{2}{mL}}\,\sin\!\left(\frac{\omega_n x}{c}\right) \qquad \text{(C-9)}$$

$$v(x,\omega) = j\omega\,\ddot{W}(\omega)\sqrt{\frac{2}{mL}}\,\sum_{n=1}^{p}\left[\frac{-\Gamma_n\,\sin\!\left(\frac{\omega_n x}{c}\right)}{(\omega_n{}^2-\omega^2)+j\left(2\xi\,\omega\omega_n\right)}\right] \qquad \text{(C-10)}$$

$$\left[v_n(x,\omega)\right]_{max} = \omega\,\ddot{W}(\omega)\sqrt{\frac{2}{mL}}\left[\frac{-\Gamma_n}{(\omega_n{}^2-\omega^2)+j\left(2\xi\,\omega\omega_n\right)}\right]_{max} \qquad \text{(C-11)}$$

The phase can be ignored.

$$\left[v_n(x,\omega)\right]_{max} = \omega\ddot{W}(\omega)\sqrt{\frac{2}{mL}}\left[\frac{-\Gamma_n}{\sqrt{(\omega_n{}^2-\omega^2)^2+(2\xi\omega\omega_n)^2}}\right] \tag{C-12}$$

A further development of the relationship between velocity and stress for this case requires that the excitation be at the natural frequency, $\omega = \omega_n$.

$$\left[\frac{\partial}{\partial x}Un(x,\omega_n)\right]_{max} = \ddot{W}(\omega_n)\frac{1}{c}\sqrt{\frac{2}{mL}}\left[\frac{-\Gamma_n\,\omega_n}{\sqrt{(\omega_n{}^2-\omega_n{}^2)^2+(2\xi\omega_n\,\omega_n)^2}}\right] \tag{C-13}$$

$$\left[\frac{\partial}{\partial x}Un(x,\omega_n)\right]_{max} = \ddot{W}(\omega_n)\frac{\Gamma_n}{2\xi\omega_n c}\sqrt{\frac{2}{mL}} \tag{C-14}$$

$$\left[v_n(x,\omega_n)\right]_{max} = \omega_n\,\ddot{W}(\omega_n)\sqrt{\frac{2}{mL}}\left[\frac{\Gamma_n}{2\xi\,\omega_n{}^2}\right] \tag{C-15}$$

$$\left[v_n(x,\omega_n)\right]_{max} = \ddot{W}(\omega_n)\left[\frac{\Gamma_n}{2\xi\,\omega_n}\right]\sqrt{\frac{2}{mL}} \tag{C-16}$$

$$\left[\frac{\partial}{\partial x}Un(x,\omega_n)\right]_{max} = \frac{1}{c}\left[v_n(x,\omega_n)\right]_{max} \tag{C-17}$$

The maximum stress is

$$\left[\sigma_n\right]_{max} = E\left[\frac{\partial}{\partial x}Un(x,\omega_n)\right]_{max} = \frac{E}{c}\left[v_n(x,\omega_n)\right]_{max} \tag{C-18}$$

APPENDIX D

Stress in a Shear Beam in Free Vibration

The following derivation is based on Reference 11.

Consider a beam which undergoes shear displacement only. Note that a shear beam model is used for seismic analysis of certain civil engineering structures.

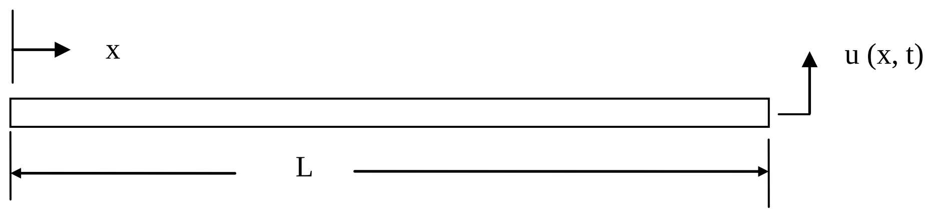

Assume a uniform cross-section and mass density.

The transverse shear displacement u(x, t) is governed by the equation

$$\rho A \frac{\partial^2 u}{\partial t^2} = KGA \frac{\partial^2 u}{\partial x^2} \tag{D-1}$$

$$\frac{\partial^2 u}{\partial t^2} = \left[\frac{KG}{\rho}\right] \frac{\partial^2 u}{\partial x^2} \tag{D-2}$$

By substitution,

$$\left[\frac{KG}{\rho}\right] \frac{\partial^2}{\partial x^2}\left[U(x)T(t)\right] = \frac{\partial^2}{\partial t^2}\left[U(x)T(t)\right] \tag{D-3}$$

Perform the partial differentiation.

$$\left[\frac{KG}{\rho}\right]U''(x)T(t) = U(x)T''(t) \tag{D-4}$$

Divide through by U(x)T(t).

$$\left[\frac{KG}{\rho}\right]\frac{U''(x)}{U(x)} = \frac{T''(t)}{T(t)} \tag{D-5}$$

Each side of equation (C-6) must equal a constant. Let ω be a constant.

$$\left[\frac{KG}{\rho}\right]\frac{U''(x)}{U(x)} = \frac{T''(t)}{T(t)} = -\omega^2 \tag{D-6}$$

The time equation is

$$\frac{T''(t)}{T(t)} = -\omega^2 \tag{D-7}$$

$$T''(t) = -\omega^2 T(t) \tag{D-8}$$

$$T''(t) + \omega^2 T(t) = 0 \tag{D-9}$$

Propose a solution

$$T(t) = a\sin(\omega t) + b\cos(\omega t) \tag{D-10}$$

$$T'(t) = a\,\omega\cos(\omega t) - b\,\omega\sin(\omega t) \tag{D-11}$$

$$T''(t) = -a\,\omega^2 \sin(\omega t) - b\,\omega^2 \cos(\omega t) \tag{D-12}$$

Verify the proposed solution. Substitute into equation (D-9).

$$-a\,\omega^2 \sin(\omega t) - b\,\omega^2 \cos(\omega t) + \omega^2\left[\sin(\omega t) + \omega^2 \cos(\omega t)\right] = 0 \tag{D-13}$$

$$0 = 0 \tag{D-14}$$

Equation (D-10) is thus verified as a solution.

There is not a unique ω , however, in equation (D-9). This is demonstrated later in the derivation. Thus a subscript n must be added as follows.

$$T_n(t) = a_n \sin(\omega_n t) + b_n \cos(\omega_n t) \tag{D-15}$$

The spatial equation is

$$\left[\frac{KG}{\rho}\right]\frac{U''(x)}{U(x)} = -\omega^2 \tag{D-16}$$

The shear wave speed is

$$c = \sqrt{\frac{KG}{\rho}} \tag{D-17}$$

$$U''(x) = -\frac{\omega^2}{c^2}\,U(x) \tag{D-18}$$

$$U''(x) + \frac{\omega^2}{c^2}\,U(x) = 0 \tag{D-19}$$

The displacement solution is

$$U(x) = d\sin\left(\frac{\omega x}{c}\right) + e\cos\left(\frac{\omega x}{c}\right) \tag{D-20}$$

The slope equation is

$$U'(x) = \left[\frac{\omega}{c}\right]\left[d\cos\left(\frac{\omega x}{c}\right) - e\sin\left(\frac{\omega x}{c}\right)\right] \tag{D-21}$$

Now consider that the shear beam is fixed-free.

The left boundary conditions is

$$u(0,t) = 0 \qquad \text{(zero displacement)} \tag{D-22}$$

$$U(0)T(t) = 0 \tag{D-23}$$

$$U(0) = 0 \tag{D-24}$$

The right boundary condition is

$$\left.\frac{\partial}{\partial x}u(x,t)\right|_{x=L} = 0 \qquad \text{(zero stress)} \tag{D-25}$$

$$U'(L)T(t) = 0 \tag{D-26}$$

$$U'(L) = 0 \tag{D-27}$$

Substitute equation (D-22) into (D-20).

$$e = 0 \tag{D-28}$$

Thus, the displacement equation becomes

$$U(x) = d \sin\left(\frac{\omega x}{c}\right) \tag{D-29}$$

$$U'(x) = \left[\frac{\omega}{c}\right]\left[d \cos\left(\frac{\omega x}{c}\right)\right] \tag{D-30}$$

Substitute equation (D-27) into equation (D-30).

$$d\cos\left(\frac{\omega L}{c}\right) = 0 \tag{D-31}$$

The constant d must be non-zero for a non-trivial solution. Thus,

$$\frac{\omega_n L}{c} = \left(\frac{2n-1}{2}\right)\pi, \quad n = 1,2,3,\ldots \tag{D-32}$$

$$\omega_n = \left(\frac{2n-1}{2}\right)\pi \frac{c}{L}, \quad n = 1,2,3,\ldots \tag{D-33}$$

The ω term is given a subscript n because there are multiple roots.

$$\omega_n = \left(\frac{2n-1}{2}\right)\pi \frac{c}{L}, \quad n = 1,2,3,\ldots \tag{D-34}$$

The displacement function for the fixed-free beam is

$$U_n(x) = d_n \sin\left(\frac{\omega_n x}{c}\right) \tag{D-35}$$

$$U_n(x) = d_n \sin\left(\frac{(2n-1)\pi x}{2L}\right) \tag{D-36}$$

$$T_n(t) = a_n \sin(\omega_n t) + b_n \cos(\omega_n t) \tag{D-37}$$

$$u(x,t) = \sum_{i=1}^{N} U_n(x) T_n(t) \tag{D-38}$$

$$u(x,t) = \sum_{i=1}^{N} \sin\left(\frac{(2n-1)\pi x}{2L}\right)\left[\hat{a}_n \sin(\omega_n t) + \hat{b}_n \cos(\omega_n t)\right] \tag{D-39}$$

$$\frac{\partial}{\partial t} u(x,t) = \sum_{i=1}^{N} \omega_n \sin\left(\frac{(2n-1)\pi x}{2L}\right)\left[\hat{a}_n \cos(\omega_n t) - \hat{b}_n \sin(\omega_n t)\right] \tag{D-40}$$

$$\omega_n = \left(\frac{2n-1}{2}\right)\pi \frac{c}{L}, \quad n = 1,2,3,\ldots \tag{D-41}$$

$$\left[\frac{\partial}{\partial t} u(x,t)\right]_{max} = \left(\frac{2n-1}{2}\right)\pi \frac{c}{L} \tag{D-42}$$

$$\frac{\partial}{\partial x} u(x,t) = \left(\frac{(2n-1)\pi}{2L}\right)\cos\left(\frac{(2n-1)\pi x}{2L}\right)\left[\hat{a}_n \sin(\omega_n t) + \hat{b}_n \cos(\omega_n t)\right] \tag{D-43}$$

$$\left[\frac{\partial}{\partial x}u(x,t)\right]_{max} = \frac{(2n-1)\pi}{2L} \tag{D-44}$$

$$\left[\frac{\partial \hat{u}_n}{\partial x}\right]_{max} = \frac{1}{c}\left[\frac{\partial \hat{u}_n}{\partial t}\right]_{max} \tag{D-45}$$

$$V = GA\frac{\partial}{\partial x}u(x,t) = GA\left(\frac{(2n-1)\pi}{2L}\right)\cos\left(\frac{(2n-1)\pi x}{2L}\right)\left[\hat{a}_n \sin(\omega_n t) + \hat{b}_n \cos(\omega_n t)\right] \tag{D-46}$$

The modal shear stress for a rectangular beam is

$$\tau_{n,max} = 1.5\frac{V_n}{A} = 1.5\ G\left[\frac{\partial}{\partial x}u_n(x,t)\right]_{max} \tag{D-47}$$

$$\tau_{n,max} = 1.5\frac{V_n}{A} = 1.5\ \frac{G}{c}\left[\frac{\partial}{\partial t}u_n(x,t)\right]_{max} \tag{D-48}$$

$$\tau_{n,max} = 1.5\ \frac{\rho c}{k}\left[\frac{\partial}{\partial t}u_n(x,t)\right]_{max} \tag{D-49}$$

The shear factors for two cross-sections are given in Table D-1, as taken from Reference 11.

Table D-1. Thomson's Shear Factors	
Cross-Section	Shear Factor K
Rectangular	2/3
Circular	3/4

APPENDIX E

Stress due to Bending in a Bernoulli-Euler Beam in Free Vibration

Consider a simply-supported beam as shown in Figure E-1.

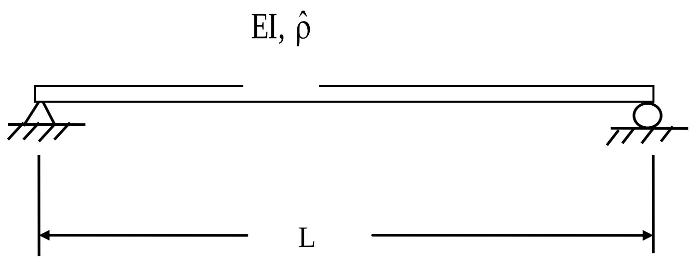

Figure E-1.

Recall that the governing differential equation is

$$-EI\frac{\partial^4 y}{\partial x^4} = \hat{\rho}\,\frac{\partial^2 y}{\partial t^2} \tag{E-1}$$

The spatial solution from Reference 12 is

$$Y(x) = a_1 \sinh(\beta x) + a_2 \cosh(\beta x) + a_3 \sin(\beta x) + a_4 \cos(\beta x) \tag{E-2}$$

$$\frac{d^2\, Y(x)}{dx^2} = a_1\beta^2 \sinh(\beta x) + a_2\beta^2 \cosh(\beta x) - a_3\beta^2 \sin(\beta x) - a_4\beta^2 \cos(\beta x) \tag{E-3}$$

The boundary conditions at the left end x = 0 are

$$Y(0) = 0 \qquad \text{(zero displacement)} \tag{E-4}$$

$$\left.\frac{d^2Y}{dx^2}\right|_{x=0} = 0 \qquad \text{(zero bending moment)} \tag{E-5}$$

The boundary conditions at the free end x = L are

$$Y(L) = 0 \qquad \text{(zero displacement)} \tag{E-6}$$

$$\left.\frac{d^2Y}{dx^2}\right|_{x=L} = 0 \qquad \text{(zero bending moment)} \tag{E-7}$$

Apply boundary condition (E-4) to (E-2).

$$a_2 + a_4 = 0 \tag{E-8}$$

$$a_4 = -a_2 \tag{E-9}$$

Apply boundary condition (E-5) to (E-3).

$$a_2 - a_4 = 0 \tag{E-10}$$

$$a_2 = a_4 \tag{E-11}$$

Equations (E-8) and (E-10) can only be satisfied if

$$a_2 = 0 \tag{E-12}$$

and

$$a_4 = 0 \tag{E-13}$$

The spatial equations thus simplify to

$$Y(x) = a_1 \sinh(\beta x) + a_3 \sin(\beta x) \tag{E-14}$$

$$\frac{d^2\, Y(x)}{dx^2} = a_1 \beta^2 \sinh(\beta x) - a_3 \beta^2 \sin(\beta x) \tag{E-15}$$

Apply boundary condition (E-6) to (E-14).

$$a_1 \sinh(\beta L) + a_3 \sin(\beta L) = 0 \tag{E-16}$$

Apply boundary condition (E-7) to (E-15).

$$a_1 \beta^2 \sinh(\beta L) - a_3 \beta^2 \sin(\beta L) = 0 \tag{E-17}$$

$$a_1 \sinh(\beta L) - a_3 \sin(\beta L) = 0 \tag{E-18}$$

$$\begin{bmatrix} \sinh(\beta L) & \sin(\beta L) \\ \sinh(\beta L) & -\sin(\beta L) \end{bmatrix} \begin{bmatrix} a_1 \\ a_3 \end{bmatrix} = \begin{bmatrix} 0 \\ 0 \end{bmatrix} \tag{E-19}$$

By inspection, equation (E-19) can only be satisfied if $a_1 = 0$ and $a_3 = 0$. Set the determinant to zero in order to obtain a nontrivial solution.

$$-\sin(\beta L)\sinh(\beta L) - \sin(\beta L)\sinh(\beta L) = 0 \tag{E-20}$$

$$-2\sin(\beta L)\sinh(\beta L)=0 \tag{E-21}$$

$$\sin(\beta L)\sinh(\beta L)=0 \tag{E-22}$$

Equation (E-22) is satisfied if

$$\beta_n L = n\pi, \quad n = 1,2,3,\ldots. \tag{E-23}$$

$$\beta_n = \frac{n\pi}{L}, \quad n = 1,2,3,\ldots. \tag{E-24}$$

The natural frequency term ω_n is

$$\omega_n = \beta_n{}^2\sqrt{\frac{EI}{\hat{\rho}}} \tag{E-25}$$

$$\omega_n = \left[\frac{n\pi}{L}\right]^2\sqrt{\frac{EI}{\hat{\rho}}}\ ,\ n = 1,2,3,\ldots \tag{E-26}$$

$$f_n = \left[\frac{1}{2\pi}\right]\left[\frac{n\pi}{L}\right]^2\sqrt{\frac{EI}{\hat{\rho}}}\ ,\ n = 1,2,3,\ldots \tag{E-27}$$

$$f_n = \left[\frac{1}{2\pi}\right]\left[\frac{n\pi}{L}\right]^2\sqrt{\frac{EI}{\hat{\rho}}}\ , \quad n = 1,2,3,\ldots \tag{E-28}$$

Normalized Eigenvectors

The eigenvector and its second derivative at this point are

$$Y(x) = a_1 \sinh(\beta x) + a_3 \sin(\beta x) \tag{E-29}$$

$$\frac{d^2 Y(x)}{dx^2} = a_1 \beta^2 \sinh(\beta x) - a_3 \beta^2 \sin(\beta x) \tag{E-30}$$

The eigenvector derivation requires some creativity. Recall

$$Y(L) = 0 \qquad \text{(zero displacement)} \tag{E-31}$$

$$\left.\frac{d^2 Y}{dx^2}\right|_{x=L} = 0 \qquad \text{(zero bending moment)} \tag{E-32}$$

Thus,

$$\frac{d^2 Y}{dx^2} + Y = 0 \quad \text{for x=L and} \quad \beta_n L = n\pi, \quad n=1,2,3, \ldots \tag{E-33}$$

$$\left(1 - \left(\frac{n\pi}{L}\right)^2\right) a_1 \sinh(n\pi) + \left(1 - \left(\frac{n\pi}{L}\right)^2\right) a_3 \sin(n\pi) = 0 \quad , n=1,2,3, \ldots \tag{E-34}$$

The sin($n\pi$) term is always zero. Thus $a_1 = 0$.

The eigenvector for all n modes is

$$Y_n(x) = a_n \sin(n\pi x / L) \tag{E-35}$$

Mass normalize the eigenvectors as follows

$$\int_0^L \hat{\rho} Y_n{}^2(x)\,dx = 1 \tag{E-36}$$

$$\hat{\rho} a_n{}^2 \int_0^L \sin^2(n\pi x / L)\,dx = 1 \tag{E-37}$$

$$\frac{\hat{\rho} a_n{}^2}{2} \int_0^L [1 - \cos(2n\,\pi x / L)] = 1 \tag{E-38}$$

$$\frac{\hat{\rho} a_n{}^2}{2} \left[x - \frac{1}{2\beta_n} \sin(2n\pi x / L) \right]_0^L = 1 \tag{E-39}$$

$$\frac{\hat{\rho} a_n{}^2\, L}{2} = 1 \tag{E-40}$$

$$a_n{}^2 = \frac{2}{\hat{\rho} L} \tag{E-41}$$

$$a_n = \sqrt{\frac{2}{\hat{\rho} L}} \tag{E-42}$$

$$Y_n(x) = \sqrt{\frac{2}{\hat{\rho} L}} \sin(n\pi\, x / L) \tag{E-43}$$

The complete solution is thus

$$y(x,t) = \sqrt{\frac{2}{\hat{\rho}L}} \sum_{i=1}^{N} \sin(n\pi x/L)\left[\hat{a}_n \sin(\omega_n t) + \hat{b}_n \cos(\omega_n t)\right] \tag{E-44}$$

$$\frac{\partial}{\partial x} y(x,t) = \frac{n\pi}{L} \sqrt{\frac{2}{\hat{\rho}L}} \sum_{i=1}^{N} \cos(n\pi x/L)\left[\hat{a}_n \sin(\omega_n t) + \hat{b}_n \cos(\omega_n t)\right] \tag{E-45}$$

$$\frac{\partial^2}{\partial x^2} y(x,t) = -\left(\frac{n\pi}{L}\right)^2 \sqrt{\frac{2}{\hat{\rho}L}} \sum_{i=1}^{N} \sin(n\pi x/L)\left[\hat{a}_n \sin(\omega_n t) + \hat{b}_n \cos(\omega_n t)\right] \tag{E-46}$$

$$\omega_n = \left[\frac{n\pi}{L}\right]^2 \sqrt{\frac{EI}{\hat{\rho}}}, n = 1,2,3,\ldots \tag{E-47}$$

$$\frac{\partial^2}{\partial x^2} y(x,t) = -\omega_n \sqrt{\frac{\hat{\rho}}{EI}} \sqrt{\frac{2}{\hat{\rho}L}} \sum_{i=1}^{N} \sin(n\pi x/L)\left[\hat{a}_n \sin(\omega_n t) + \hat{b}_n \cos(\omega_n t)\right] \tag{E-48}$$

$$\left[\frac{\partial^2}{\partial x^2} y_n(x,t)\right]_{max} = \omega_n \sqrt{\frac{\hat{\rho}}{EI}} \sqrt{\frac{2}{\hat{\rho}L}} \tag{E-49}$$

$$\left[\frac{\partial}{\partial t} y_n(x,t)\right]_{max} = \omega_n \sqrt{\frac{2}{\hat{\rho}L}} \tag{E-50}$$

$$\left[\frac{\partial^2}{\partial x^2} y_n(x,t)\right]_{max} = \sqrt{\frac{\hat{\rho}}{EI}} \left[\frac{\partial}{\partial t} y_n(x,t)\right]_{max} \tag{E-51}$$

$$\left[\frac{\partial^2}{\partial x^2} y_n(x,t)\right]_{max} = \sqrt{\frac{\rho A}{EI}} \left[\frac{\partial}{\partial t} y_n(x,t)\right]_{max} \tag{E-52}$$

Let c_L be the longitudinal wave speed in the material.

$$c_L = \sqrt{\frac{E}{\rho}} \tag{E-53}$$

$$\left[\frac{\partial^2}{\partial x^2} y_n(x,t)\right]_{max} = \frac{1}{c_L}\sqrt{\frac{A}{I}} \left[\frac{\partial}{\partial t} y_n(x,t)\right]_{max} \tag{E-54}$$

$$M_{max} = EI\left[\frac{\partial^2}{\partial x^2} y_n(x,t)\right]_{max} = \frac{EI}{c_L}\sqrt{\frac{A}{I}} \left[\frac{\partial}{\partial t} y_n(x,t)\right]_{max} \tag{E-55}$$

$$\sigma_{max} = \frac{M_{max}\ \hat{c}}{I} \tag{E-56}$$

$$\sigma_{max} = E\,\hat{c}\left[\frac{\partial^2}{\partial x^2} y_n(x,t)\right]_{max} = \frac{E\ \hat{c}}{c_L}\sqrt{\frac{A}{I}} \left[\frac{\partial}{\partial t} y_n(x,t)\right]_{max} \tag{E-57}$$

$$\sigma_{max} = E\,\hat{c}\left[\frac{\partial^2}{\partial x^2}\,y_n(x,t)\right]_{max} = \hat{c}\,\sqrt{\frac{EA\rho}{I}}\,\left[\frac{\partial}{\partial t}\,y_n(x,t)\right]_{max} \qquad \text{(E-58)}$$

APPENDIX F

<u>Stress due to Bending in a Bernoulli-Euler Beam Excited by Base Excitation</u>

Consider a beam simply-supported at each end subjected to base excitation.

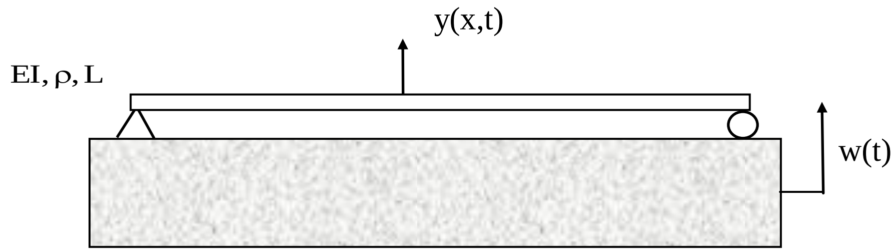

Figure F-1.

The following is taken from Reference 16.

The governing differential equation is

$$EI\frac{\partial^4 y}{\partial x^4} + \hat{\rho}\frac{\partial^2 y}{\partial t^2} = -\hat{\rho}\frac{\partial^2 w}{\partial t^2} \quad \text{(F-1)}$$

The mass-normalized mode shapes are

$$Y_n(x) = \sqrt{\frac{2}{\hat{\rho}L}}\sin(\beta_n x) \quad \text{(F-2)}$$

$$\frac{d^2}{dx^2}Y_n(x) = -\beta_n{}^2\sqrt{\frac{2}{\hat{\rho}L}}\sin(\beta_n x) \quad \text{(F-3a)}$$

$$\frac{d^2}{dx^2}Y_n(x) = -\beta_n{}^2\,Y_n(x) \quad \text{(F-3b)}$$

The eigenvalues are

$$\beta_n = \frac{n\pi}{L}, \quad n = 1, 2, 3, \ldots \tag{F-4}$$

The natural frequencies are

$$\omega_n = \beta_n{}^2 \sqrt{EI/\hat{\rho}} \tag{F-5}$$

The relative displacement response Y(x, ω) to base acceleration is

$$Y(x,\omega) = \ddot{W}(\omega) \sum_{n=1}^{m} \left\{ \frac{-\Gamma_n Y_n(x)}{(\omega_n^2 - \omega^2) + j2\xi_n \omega\omega_n} \right\} \tag{F-6}$$

$$\frac{\partial^2}{\partial x^2} Y(x,\omega) = \ddot{W}(\omega) \sum_{n=1}^{m} \left\{ \frac{-\Gamma_n \dfrac{d^2}{dx^2} Y_n(x)}{(\omega_n^2 - \omega^2) + j2\xi_n \omega\omega_n} \right\} \tag{F-7}$$

$$\frac{\partial^2}{\partial x^2} Y(x,\omega) = \ddot{W}(\omega) \sum_{n=1}^{m} \left\{ \frac{\Gamma_n \ \beta_n{}^2 \ Y_n(x)}{(\omega_n^2 - \omega^2) + j2\xi_n \omega\omega_n} \right\} \tag{F-8}$$

On a modal basis,

$$\left[\frac{\partial^2}{\partial x^2} Y_n(x,\omega) \right]_{max} = \ddot{W}(\omega) \left[\frac{\Gamma_n \ \beta_n{}^2}{(\omega_n^2 - \omega^2) + j2\xi_n \omega\omega_n} \right] [Y_n(x)]_{max} \tag{F-9}$$

The phase can be ignored.

$$\left[\frac{\partial^2}{\partial x^2} Y_n(x,\omega)\right]_{max} = \ddot{W}(\omega)\left[\frac{\Gamma_n \ \beta_n{}^2}{\sqrt{(\omega_n{}^2 - \omega^2)^2 + (2\xi\omega\omega_n)^2}}\right][Y_n(x)]_{max} \qquad \text{(F-10)}$$

The relative velocity v in the frequency domain is

$$v(x,\omega) = j\omega\ddot{W}(\omega)\sum_{n=1}^{m}\left\{\frac{-\Gamma_n Y_n(x)}{(\omega_n^2 - \omega^2) + j2\xi_n\omega\omega_n}\right\} \qquad \text{(F-11)}$$

On a modal basis,

$$[v(x,\omega)]_{max} = j\omega\ddot{W}(\omega)\left[\frac{-\Gamma_n}{(\omega_n^2 - \omega^2) + j2\xi_n\omega\omega_n}\right][Y_n(x)]_{max} \qquad \text{(F-12)}$$

The phase can be ignored.

$$[v(x,\omega)]_{max} = \omega\ddot{W}(\omega)\left[\frac{\Gamma_n}{\sqrt{(\omega_n{}^2 - \omega^2)^2 + (2\xi\omega\omega_n)^2}}\right][Y_n(x)]_{max} \qquad \text{(F-13)}$$

The second derivative and velocity are related by

$$\left[\frac{\partial^2}{\partial x^2} Y_n(x,\omega)\right]_{max} = \frac{\beta_n{}^2}{\omega}[v(x,\omega)]_{max} \qquad \text{(F-14)}$$

$$\omega_n = \beta_n{}^2 \sqrt{EI/\hat{\rho}} \tag{F-15}$$

$$\left[\frac{\partial^2}{\partial x^2} Y_n(x,\omega) \right]_{max} = \frac{\omega_n}{\omega} \sqrt{\frac{\hat{\rho}}{EI}} \, [v(x,\omega)]_{max} \tag{F-16}$$

Note consider the case where $\omega = \omega_n$.

$$\left[\frac{\partial^2}{\partial x^2} Y_n(x,\omega_n) \right]_{max} = \sqrt{\frac{\hat{\rho}}{EI}} \, [v(x,\omega)]_{max} \tag{F-17}$$

$$\left[\frac{\partial^2}{\partial x^2} Y_n(x,\omega_n) \right]_{max} = \frac{1}{c_L \sqrt{I}} \, [v(x,\omega)]_{max} \tag{F-18}$$

The bending moment is

$$M_{max} = EI \left[\frac{\partial^2}{\partial x^2} Y_n(x,\omega_n) \right]_{max} = \frac{E\sqrt{I}}{c_L} \, [v(x,\omega)]_{max} \tag{F-19}$$

$$M_{max} = EI \left[\frac{\partial^2}{\partial x^2} Y_n(x,\omega_n) \right]_{max} = \sqrt{EAI\rho} \, [v(x,\omega)]_{max} \tag{F-20}$$

The bending stress is

$$\sigma_{max} = E\hat{c}\left[\frac{\partial^2}{\partial x^2} Y_n(x,\omega_n)\right]_{max} = \hat{c}\sqrt{\frac{EA\rho}{I}}\,[v(x,\omega)]_{max} \tag{F-21}$$

This concept can be extended to the multi-modal response for the special case of simply-supported beam.

Again,

$$\frac{\partial^2}{\partial x^2} Y(x,\omega) = \ddot{W}(\omega)\sum_{n=1}^{m}\left\{\frac{\Gamma_n\ \beta_n{}^2\ Y_n(x)}{(\omega_n^2-\omega^2)+j2\xi_n\omega\omega_n}\right\} \tag{F-22}$$

$$v(x,\omega) = j\omega\ddot{W}(\omega)\sum_{n=1}^{m}\left\{\frac{-\Gamma_n Y_n(x)}{(\omega_n^2-\omega^2)+j2\xi_n\omega\omega_n}\right\} \tag{F-23}$$

Thus

$$\frac{\partial^2}{\partial x^2} Y(x,\omega) = \frac{-\beta_n{}^2}{j\omega} v(x,\omega) \tag{F-24}$$

$$\frac{\partial^2}{\partial x^2} Y(x,\omega) = \frac{j\beta_n{}^2}{\omega} v(x,\omega) \tag{F-25}$$

Now consider a fixed-free beam subjected to base excitation.

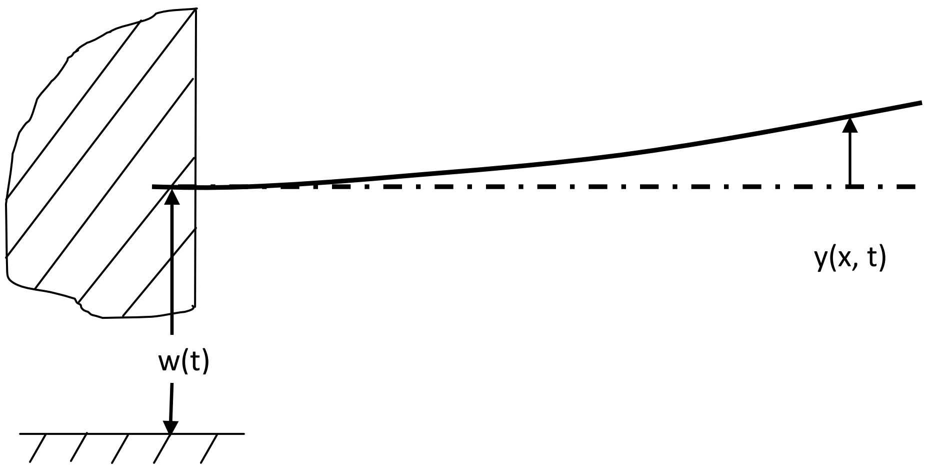

Figure F-2.

The eigenvalues are

n	$\beta_n L$
1	1.875104
2	4.69409
3	7.85476
4	10.99554
5	$(2n-1)\pi/2$

Note that the root value formula for n $\geq$ 5 is approximate.

The natural frequencies are

$$\omega_n = \beta_n{}^2 \sqrt{EI/\hat{\rho}} \tag{F-26}$$

The mass-normalized mode shapes can be represented as

$$Y_i(x) = \left\{\frac{1}{\sqrt{\rho L}}\right\}\{[\cosh(\beta_i x) - \cos(\beta_i x)] - D_i\ [\sinh(\beta_i x) - \sin(\beta_i x)]\} \tag{F-27}$$

where

$$D_i = \frac{\cos(\beta_i L) + \cosh(\beta_i L)}{\sin(\beta_i L) + \sinh(\beta_i L)} \tag{F-28}$$

$$Y_i'(x) = \left\{\frac{\beta_i}{\sqrt{\rho L}}\right\}\{[\sinh(\beta_i x) + \sin(\beta_i x)] - D_i\ [\cosh(\beta_i x) - \cos(\beta_i x)]\} \tag{F-29}$$

$$Y_i''(x) = \left\{\frac{\beta_i^{\,2}}{\sqrt{\rho L}}\right\}\{[\cosh(\beta_i x) + \cos(\beta_i x)] - D_i\ [\sinh(\beta_i x) + \sin(\beta_i x)]\} \tag{F-30}$$

$$Y_i^{III}(x) = \left\{\frac{\beta_i^{\,3}}{\sqrt{\rho L}}\right\}\{[\sinh(\beta_i x) - \sin(\beta_i x)] - D_i\ [\cosh(\beta_i x) + \cos(\beta_i x)]\} \tag{F-31}$$

Note that

$$Y_i(L) = \left\{\frac{1}{\sqrt{\rho L}}\right\}\left\{[\cosh(\beta_i L) - \cos(\beta_i L)] - \left[\frac{\cos(\beta_i L) + \cosh(\beta_i L)}{\sin(\beta_i L) + \sinh(\beta_i L)}\right][\sinh(\beta_i L) - \sin(\beta_i L)]\right\} \tag{F-32}$$

n	$\beta_n L$	$Y_i(L)$
1	1.875104	$2\sqrt{\rho L}$
2	4.69409	$-2\sqrt{\rho L}$
3	7.85476	$2\sqrt{\rho L}$
4	10.99554	$-2\sqrt{\rho L}$

Thus,

$$Y_1''(0) = \beta_1{}^2 Y_1(L) \tag{F-33}$$

The relative displacement response Y(x, ω) to base acceleration is

$$Y(x,\omega) = \ddot{W}(\omega) \sum_{n=1}^{m} \left\{ \frac{-\Gamma_n Y_n(x)}{(\omega_n^2 - \omega^2) + j2\xi_n \omega\omega_n} \right\} \tag{F-34}$$

$$\frac{\partial^2}{\partial x^2} Y(x,\omega) = \ddot{W}(\omega) \sum_{n=1}^{m} \left\{ \frac{-\Gamma_n \dfrac{d^2}{dx^2} Y_n(x)}{(\omega_n^2 - \omega^2) + j2\xi_n \omega\omega_n} \right\} \tag{F-35}$$

On a modal basis,

$$\left[\frac{\partial^2}{\partial x^2} Y_n(x,\omega) \right]_{max} = \ddot{W}(\omega) \left\{ \frac{-\Gamma_n \dfrac{d^2}{dx^2} Y_n(x)}{(\omega_n^2 - \omega^2) + j2\xi_n \omega\omega_n} \right\}_{max} \tag{F-36}$$

The maximum occurs at x=0. Solve for the first mode.

$$\left[\frac{\partial^2}{\partial x^2} Y_1(0,\omega)\right] = \ddot{W}(\omega)\left\{\frac{-\Gamma_1 \frac{d^2}{dx^2} Y_1(0)}{(\omega_1^2 - \omega^2) + j2\xi_1\omega\omega_1}\right\} \tag{F-37}$$

$$\left[\frac{\partial^2}{\partial x^2} Y_1(0,\omega)\right] = \ddot{W}(\omega)\left\{\frac{-\Gamma_1 \beta_1^2}{(\omega_1^2 - \omega^2) + j2\xi_1\omega\omega_1}\right\}[Y_1(L)] \tag{F-38}$$

The phase can be ignored.

$$\left[\frac{\partial^2}{\partial x^2} Y_L(0,\omega)\right] = \ddot{W}(\omega)\left[\frac{\Gamma_1 \beta_1^2}{\sqrt{(\omega_1^2 - \omega^2)^2 + (2\xi_1 \omega\omega_1)^2}}\right][Y_1(L)] \tag{F-39}$$

The relative velocity v in the frequency domain is

$$v(x,\omega) = j\omega\ddot{W}(\omega)\sum_{n=1}^{m}\left\{\frac{-\Gamma_n Y_n(x)}{(\omega_n^2 - \omega^2) + j2\xi_n\omega\omega_n}\right\} \tag{F-40}$$

The first modal velocity is

$$[v(x,\omega)]_{max} = j\omega\ddot{W}(\omega)\left[\frac{-\Gamma_1}{(\omega_1^2 - \omega^2) + j2\xi_1\omega\omega_1}\right][Y_n(x)]_{max} \tag{F-41}$$

The phase can be ignored.

$$\left[v(x,\omega)\right]_{max} = \omega \ddot{W}(\omega)\left[\frac{\Gamma_1}{\sqrt{(\omega_1{}^2-\omega^2)^2+\left(2\xi_1\,\omega\,\omega_1\right)^2}}\right]\left[Y_1(x)\right]_{max} \tag{F-42}$$

The maximum velocity occurs at x=L.

$$v(L,\omega) = \omega \ddot{W}(\omega)\left[\frac{\Gamma_1}{\sqrt{(\omega_1{}^2-\omega^2)^2+\left(2\xi_1\,\omega\,\omega_1\right)^2}}\right]Y_1(L) \tag{F-43}$$

$$\frac{\partial^2}{\partial x^2}Y_L(0,\omega) = \frac{\beta_1{}^2}{\omega}v(L,\omega) \tag{F-44}$$

The bending moment is

$$M(0,\omega) = EI\frac{\partial^2}{\partial x^2}Y_L(0,\omega) = EI\frac{\beta_1{}^2}{\omega}v(L,\omega) \tag{F-45}$$

The bending stress is

$$\sigma_{max} = \hat{c}\,E\left[\frac{\partial^2}{\partial x^2}Y_n(0,\omega)\right] = \hat{c}\,E\frac{\beta_1{}^2}{\omega}v(L,\omega) \tag{F-46}$$

APPENDIX G

Stress in a Rectangular Plate in Free Vibration

Consider the rectangular plate in Figure 1.

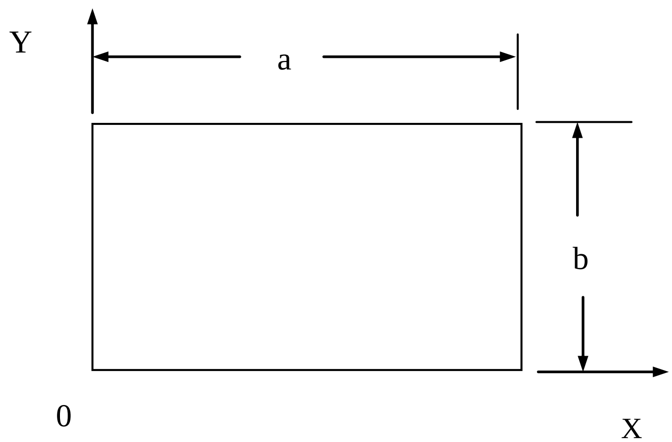

Figure G-1.

The governing equation of motion from Reference 14 is

$$D\left(\frac{\partial^4 z}{\partial x^4}+2\frac{\partial^4 z}{\partial x^2 \partial y^2}+\frac{\partial^4 z}{\partial y^4}\right)+\rho h\frac{\partial^2 z}{\partial t^2}=0 \tag{G-1}$$

Assume a harmonic response.

$$z(x,y,t)=\sum_{m=1}^{M}\sum_{n=1}^{N} Z_{mn}(x,y)\exp(j\omega t) \tag{G-2}$$

The modal displacement for a plate simply-supported on all four edges is

$$Z_{mn}=A_{mn}\sin\left(\frac{m\pi x}{a}\right)\sin\left(\frac{n\pi y}{b}\right) \tag{G-3}$$

The natural frequencies are

$$\omega_{mn} = \sqrt{\frac{D}{\rho h}} \left(\left(\frac{m\pi}{a} \right)^2 + \left(\frac{n\pi}{b} \right)^2 \right) \tag{G-4}$$

The partial derivates are

$$\frac{\partial}{\partial x} Z_{mn} = \left(\frac{m\pi}{a} \right) A_{mn} \cos\left(\frac{m\pi x}{a} \right) \sin\left(\frac{n\pi y}{b} \right) \tag{G-5}$$

$$\frac{\partial^2}{\partial x^2} Z_{mn} = -\left(\frac{m\pi}{a} \right)^2 A_{mn} \sin\left(\frac{m\pi x}{a} \right) \sin\left(\frac{n\pi y}{b} \right) \tag{G-6}$$

$$\frac{\partial}{\partial y} Z_{mn} = \left(\frac{n\pi}{b} \right) A_{mn} \sin\left(\frac{m\pi x}{a} \right) \cos\left(\frac{n\pi y}{b} \right) \tag{G-7}$$

$$\frac{\partial^2}{\partial y^2} Z_{mn} = -\left(\frac{n\pi}{b} \right)^2 A_{mn} \sin\left(\frac{m\pi x}{a} \right) \sin\left(\frac{n\pi y}{b} \right) \tag{G-8}$$

The modal bending moments are

$$M_{mn,x} = -D\left(\frac{\partial^2}{\partial x^2} Z_{mn} + \nu \frac{\partial^2}{\partial y^2} Z_{mn} \right) \tag{G-9}$$

$$M_{mn,y} = -D\left(\nu \frac{\partial^2}{\partial x^2} Z_{mn} + \frac{\partial^2}{\partial y^2} Z_{mn} \right) \tag{G-10}$$

The maximum modal stress at any given cross section is

$$\sigma_{mn,x} = \frac{6}{h^2} M_{mn,x} = -\frac{6D}{h^2}\left(\frac{\partial^2}{\partial x^2} Z_{mn} + \nu \frac{\partial^2}{\partial y^2} Z_{mn} \right) \tag{G-11}$$

$$\sigma_{mn,y} = \frac{6}{h^2} M_{mn,x} = -\frac{6D}{h^2}\left(\frac{\partial^2}{\partial y^2} Z_{mn} + \nu \frac{\partial^2}{\partial x^2} Z_{mn} \right) \tag{G-12}$$

The total maximum modal stress for any mode is

$$\left[\sigma_{mn,x}\right]_{max} = \frac{6DA_{mn}}{h^2}\left[\left(\frac{m\pi}{a}\right)^2 + \nu \left(\frac{n\pi}{b}\right)^2 \right] \tag{G-13}$$

$$\left[\sigma_{mn,y}\right]_{max} = \frac{6DA_{mn}}{h^2}\left[\left(\frac{n\pi}{b}\right)^2 + \nu \left(\frac{m\pi}{a}\right)^2 \right] \tag{G-14}$$

Note that

$$\frac{\partial}{\partial t} Z_{mn} = \omega A_{mn} \sin\left(\frac{m\pi x}{a}\right) \sin\left(\frac{n\pi y}{b}\right) \tag{G-15}$$

For free vibration, $\omega = \omega_{mn}$

$$\frac{\partial}{\partial t} Z_{mn} = \omega_{mn} A_{mn} \sin\left(\frac{m\pi x}{a}\right) \sin\left(\frac{n\pi y}{b}\right) \tag{G-16}$$

$$\frac{\partial}{\partial t} Z_{mn} = \omega_{mn} A_{mn} \sin\left(\frac{m\pi x}{a}\right) \sin\left(\frac{n\pi y}{b}\right) \tag{G-17}$$

$$\omega_{mn} = \sqrt{\frac{D}{\rho h}} \left(\left(\frac{m\pi}{a}\right)^2 + \left(\frac{n\pi}{b}\right)^2 \right) \tag{G-18}$$

The velocity is

$$\frac{\partial}{\partial t} Z_{mn} = \sqrt{\frac{D}{\rho h}} \left(\left(\frac{m\pi}{a}\right)^2 + \left(\frac{n\pi}{b}\right)^2 \right) A_{mn} \sin\left(\frac{m\pi x}{a}\right) \sin\left(\frac{n\pi y}{b}\right) \tag{G-19}$$

$$\left[\frac{\partial}{\partial t} Z_{mn}\right]_{max} = \sqrt{\frac{D}{\rho h}} \left(\left(\frac{m\pi}{a}\right)^2 + \left(\frac{n\pi}{b}\right)^2 \right) A_{mn} \tag{G-20}$$

<u>Intermodal Segment</u>

Consider a higher mode. The vibration mode for an intermodal segment can be represent with n=m=1.

Hunt in Reference 1 notes:

> It is relatively more difficult to establish equally general relations between antinodal velocity and extensionally strain for a thin plate vibrating transversely, owing to the more complex boundary conditions and the Poisson coupling between the principal stresses. One can deal, however, with the velocity strain relations in the interior of such a plate by invoking again the fact that conditions along an interior nodal line correspond to those of a simple edge support. Each intermodal segment can, therefore, be treated as if it were a simply supported rectangular plate of dimensions Lx, Ly vibrating in its fundamental mode, where Lx and Ly are the nodal separations along the X and Y axes, as shown in Figure G-2.

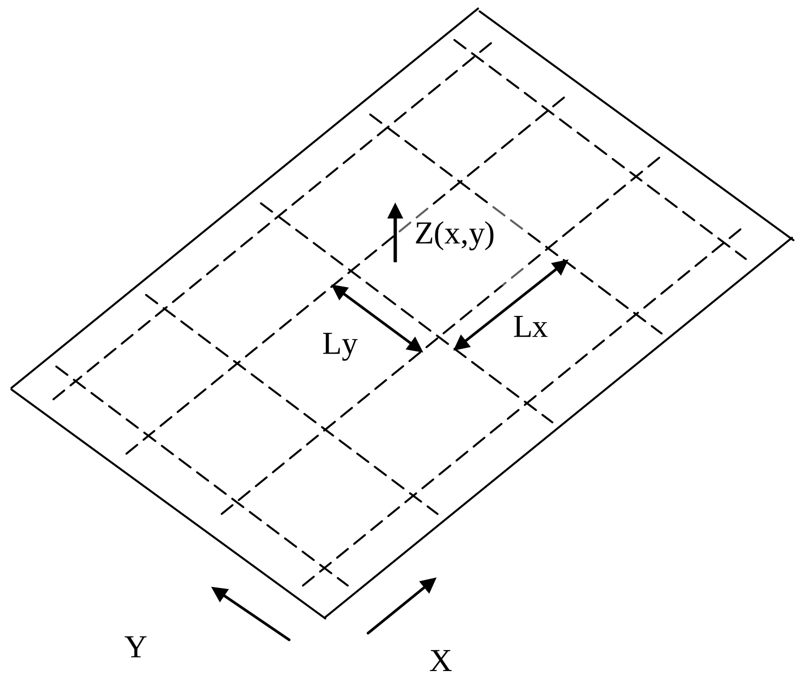

Figure 2. Rectangular Plate Vibrating in a Higher-order Model

The dashed lines are the nodal lines. An intermodal segment is isolated for analysis as a plate of dimension Lx, Ly with simply-supported edges vibrating in its intermodal fundamental mode.

The subscript *int* is used to denote intermodal segment.

$$\left[\sigma_{int,x}\right]_{max} = \frac{6DA_{int}}{h^2}\left[\left(\frac{\pi}{L_x}\right)^2 + \nu\left(\frac{\pi}{L_y}\right)^2\right] \tag{G-21}$$

$$\left[\sigma_{int,y}\right]_{max} = \frac{6DA_{int}}{h^2}\left[\left(\frac{\pi}{L_y}\right)^2 + \nu\left(\frac{\pi}{L_x}\right)^2\right] \tag{G-22}$$

$$\left[\frac{\partial}{\partial t} Z_{int}\right]_{max} = \sqrt{\frac{D}{\rho h}} \left(\left(\frac{\pi}{L_x}\right)^2 + \left(\frac{\pi}{L_y}\right)^2\right) A_{int} \tag{G-23}$$

$$A_{int} = \frac{\left[\frac{\partial}{\partial t} Z_{int}\right]_{max}}{\sqrt{\frac{D}{\rho h}} \left(\left(\frac{\pi}{L_x}\right)^2 + \left(\frac{\pi}{L_y}\right)^2\right)} \tag{G-24}$$

$$\left[\sigma_{int,x}\right]_{max} = \frac{6D}{h^2} \left[\frac{\partial}{\partial t} Z_{int}\right]_{max} \frac{\left[\left(\frac{\pi}{L_x}\right)^2 + \nu\left(\frac{\pi}{L_y}\right)^2\right]}{\sqrt{\frac{D}{\rho h}} \left(\left(\frac{\pi}{L_x}\right)^2 + \left(\frac{\pi}{L_y}\right)^2\right)} \tag{G-25}$$

$$\left[\sigma_{int,x}\right]_{max} = \frac{6\sqrt{D\rho h}}{h^2} \left[\frac{\partial}{\partial t} Z_{int}\right]_{max} \left[\frac{\left(\frac{\pi}{L_x}\right)^2 + \nu\left(\frac{\pi}{L_y}\right)^2}{\left(\frac{\pi}{L_x}\right)^2 + \left(\frac{\pi}{L_y}\right)^2}\right] \tag{G-26}$$

The plate stiffness factor is

$$D = \frac{Eh^3}{12\,(1-\nu^2)} \tag{G-27}$$

$$\left[\sigma_{int,x}\right]_{max} = \frac{6\sqrt{\dfrac{Eh^4\rho}{12\,(1-\nu^2)}}}{h^2}\left[\frac{\partial}{\partial t}Z_{int}\right]_{max}\left[\frac{\left(\dfrac{\pi}{L_x}\right)^2+\nu\left(\dfrac{\pi}{L_y}\right)^2}{\left(\dfrac{\pi}{L_x}\right)^2+\left(\dfrac{\pi}{L_y}\right)^2}\right] \tag{G-28}$$

$$\left[\sigma_{int,x}\right]_{max} = 6\sqrt{\frac{E\rho}{12\,(1-\nu^2)}}\left[\frac{\partial}{\partial t}Z_{int}\right]_{max}\left[\frac{\left(\dfrac{\pi}{L_x}\right)^2+\nu\left(\dfrac{\pi}{L_y}\right)^2}{\left(\dfrac{\pi}{L_x}\right)^2+\left(\dfrac{\pi}{L_y}\right)^2}\right] \tag{G-29}$$

$$\left[\sigma_{int,x}\right]_{max} = \sqrt{\frac{3E\rho}{1-\nu^2}}\left[\frac{\partial}{\partial t}Z_{int}\right]_{max}\left[\frac{(\pi L_y)^2+\nu(\pi L_x)^2}{(\pi L_y)^2+(\pi L_x)^2}\right] \tag{G-30}$$

$$\left[\sigma_{int,x}\right]_{max} = \sqrt{\frac{3E\rho}{1-\nu^2}}\left[\frac{\partial}{\partial t}Z_{int}\right]_{max}\left[\frac{L_y{}^2+\nu L_x{}^2}{L_y{}^2+L_x{}^2}\right] \tag{G-31}$$

$$\left[\sigma_{int,x}\right]_{max} = \rho c \sqrt{\frac{3}{1-\nu^2}} \left[\frac{\partial}{\partial t} Z_{int}\right]_{max} \left[\frac{L_y{}^2 + \nu L_x{}^2}{L_y{}^2 + L_x{}^2}\right] \tag{G-32}$$

Similarly,

$$\left[\sigma_{int,y}\right]_{max} = \rho c \sqrt{\frac{3}{1-\nu^2}} \left[\frac{\partial}{\partial t} Z_{int}\right]_{max} \left[\frac{L_x{}^2 + \nu L_y{}^2}{L_y{}^2 + L_x{}^2}\right] \tag{G-33}$$

APPENDIX H

MIL-STD-810E

An empirical rule-of-thumb in MIL-STD-810E states that a shock response spectrum is considered severe only if one of its components exceeds the level

$$\text{Threshold} = [\ 0.8\ (\text{G/Hz}) * \text{Natural Frequency (Hz)}\ ] \tag{H-1}$$

For example, the severity threshold at 100 Hz would be 80 G.

This rule is effectively a velocity criterion.

MIL-STD-810E states that it is based on unpublished observations that military-quality equipment does not tend to exhibit shock failures below a shock response spectrum velocity of 100 inches/sec (254 cm/sec).

Equation (H-1) actually corresponds to 50 inches/sec. It thus has a built-in 6 dB margin of conservatism.

Note that this rule was not included in MIL-STD-810F or G, however.

Morse Chart

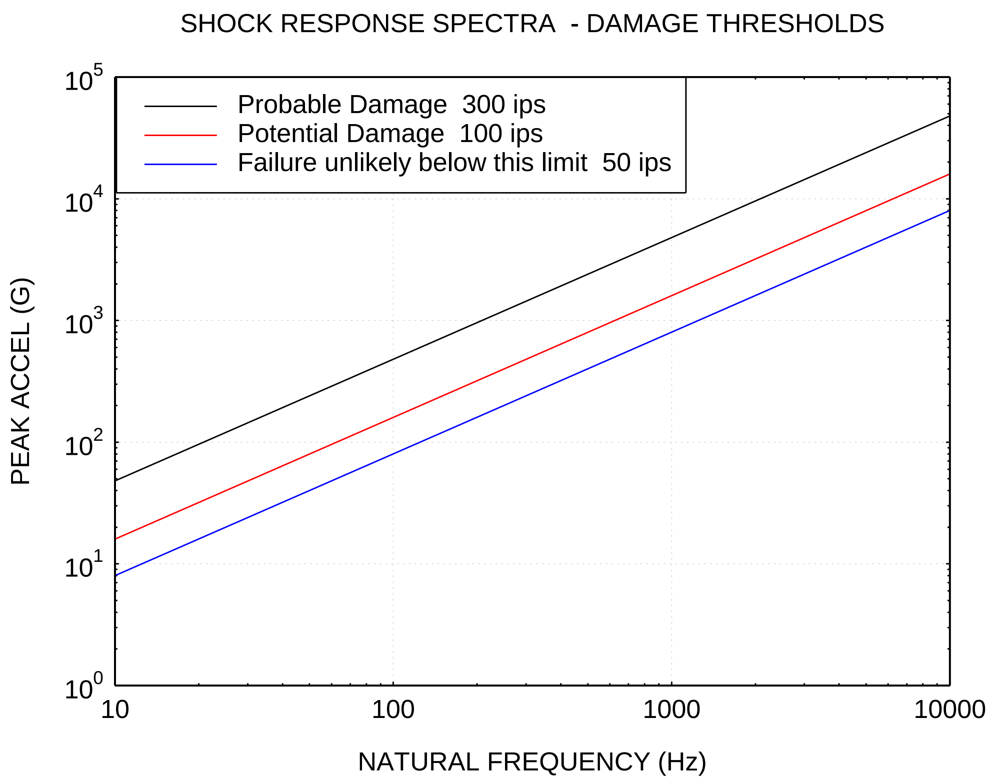

Figure H-1.

The curves in Figure H-1 are taken from Reference 30. The curves are defined by the following formulas.

Threshold	Formula
300 ips	[4.8 (G/Hz) * Natural Frequency (Hz)]
100 ips	[1.6 (G/Hz) * Natural Frequency (Hz)]
50 ips	[0.8 (G/Hz) * Natural Frequency (Hz)]

The 100 ips threshold is defined in part by the observation that the severe velocities which cause yield point stresses in mild steel beams turn out to be about 130 ips, per Reference 29.

APPENDIX I

MIL-STD-810G, METHOD 516.6

A more complete description of the shock (potentially more useful for shock damage assessment, but not widely accepted) can be obtained by determining the maximax pseudo-velocity response spectrum and plotting this on four-coordinate paper where, in pairs of orthogonal axes, the maximax pseudo-velocity response spectrum is represented by the ordinate, with the undamped natural frequency being the abscissa and the maximax absolute acceleration along with maximax pseudo-displacement plotted in a pair of orthogonal axes, all plots having the same abscissa.

The maximax pseudo-velocity at a particular SDOF undamped natural frequency is thought to be more representative of the damage potential for a shock since it correlates with stress and strain in the elements of a single degree of freedom system (paragraph 6.1, reference f). If the testing is to be used for laboratory simulation, use 516.6-8 a Q value of ten and a second Q value of 50 in the processing. Using two Q values, a damped value and a value corresponding to light damping, provides an analyst with information on the potential spread of materiel response.

It is recommended that the maximax absolute acceleration SRS be the primary method of display for the shock, with the maximax pseudo-velocity SRS the secondary method of display and useful in cases in which it is desirable to be able to correlate damage of simple systems with the shock.

(End Quote)

Note that Reference f is:

Harris, C., and C. E. Crede, eds., Shock and Vibration Handbook, 5th Edition, NY, McGraw-Hill, 2001.

APPENDIX J

Pseudo Velocity Shock Response Spectrum

The Shock Response Spectrum (SRS) models the peak response of a single-degree-of-freedom (SDOF) system to a base acceleration, where the system's natural frequency is an independent variable. The SRS method is thoroughly covered in Reference 15. The purpose of this appendix is to present some additional notes.

The absolute acceleration and the relative displacement of the SDOF system can be readily calculated.

The velocity, however, is more difficult to calculate accurately.

The "pseudo velocity" is an approximation of the relative velocity.

The peak pseudo velocity is equal to the peak relative displacement multiplied by the natural frequency ω_n which has units of radians per second.

The peak pseudo acceleration is equal to the peak relative displacement multiplied by the natural frequency ω_n^2.

The peak pseudo acceleration is thus equal to the peak pseudo velocity multiplied by the natural frequency ω_n. There may be little reason if any to calculate pseudo acceleration in practice, however, because the absolute acceleration can be calculated directly.

Furthermore, one of the advantages of the pseudo velocity SRS is that it tends to produce a more uniform SRS than either acceleration or relative displacement.

Additional information is given in Reference 16.

APPENDIX K

<u>Half-Sine Pulse</u>

SRS Q=10, Half-Sine Pulse, 10 G, 11 msec

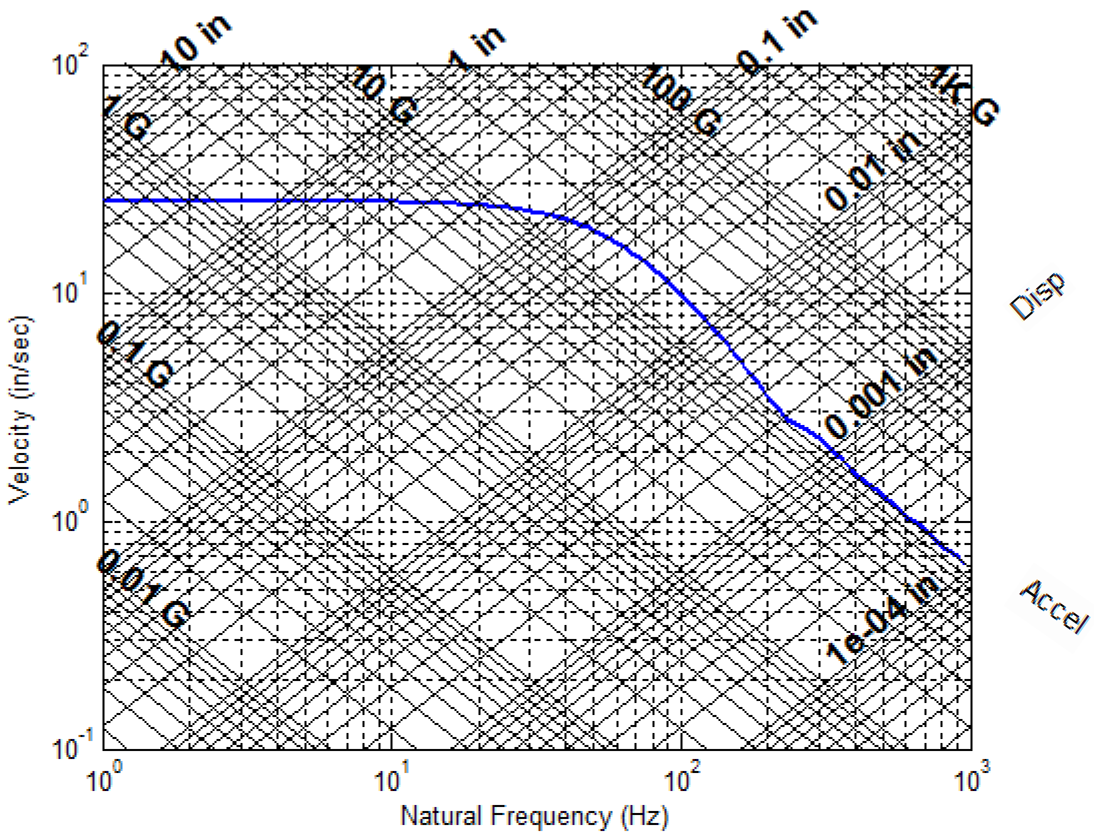

Figure K-1.

Table K-1. SRS Q=10, Half-Sine Pulse, 10 G, 11 msec, 1 to 1000 Hz			
Parameter	Max	Min	Range (dB)
Displacement (inch)	4.0	1.1e-04	91
Velocity (in/sec)	25.2	0.64	32
Acceleration (G)	16.5	0.41	32

The velocity and acceleration spectra have the same range in terms of decibels.

APPENDIX L

El Centro Earthquake

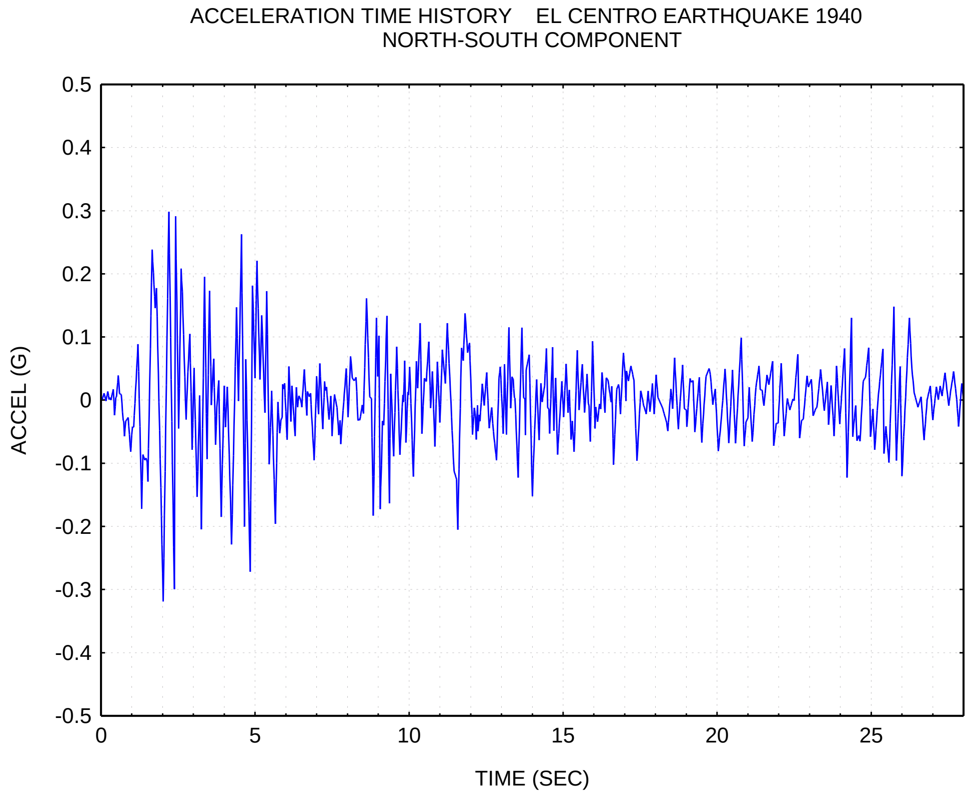

Figure L-1.

El Centro (Imperial Valley) Earthquake

Nine people were killed by the May 1940 Imperial Valley earthquake. At Imperial, 80 percent of the buildings were damaged to some degree. In the business district of Brawley, all structures were damaged, and about 50 percent had to be condemned. The shock caused 40 miles of surface faulting on the Imperial Fault, part of the San Andreas system in southern California. It was the first strong test of public schools designed to be earthquake-resistive after the 1933 Long Beach quake. Fifteen such public schools in the area had no apparent damage. Total damage has been estimated at about $6 million. The magnitude was 7.1.

The El Centro earthquake was the first major quake in which calibrated, strong-motion source data was measured which would be useful for engineering purposes. This data has obvious application to the design of building, bridges, and dams in California. It also has some surprising aerospace uses. Consider a rocket vehicle mounted as a cantilever beam to a launch pad at Vandenberg AFB on the central California coast. Engineers must verify that the vehicle can withstand a hypothetical seismic event prior to launch. The El Centro earthquake data has thus been used in some analyses as a modal transient input to the rocket vehicle's finite element model.

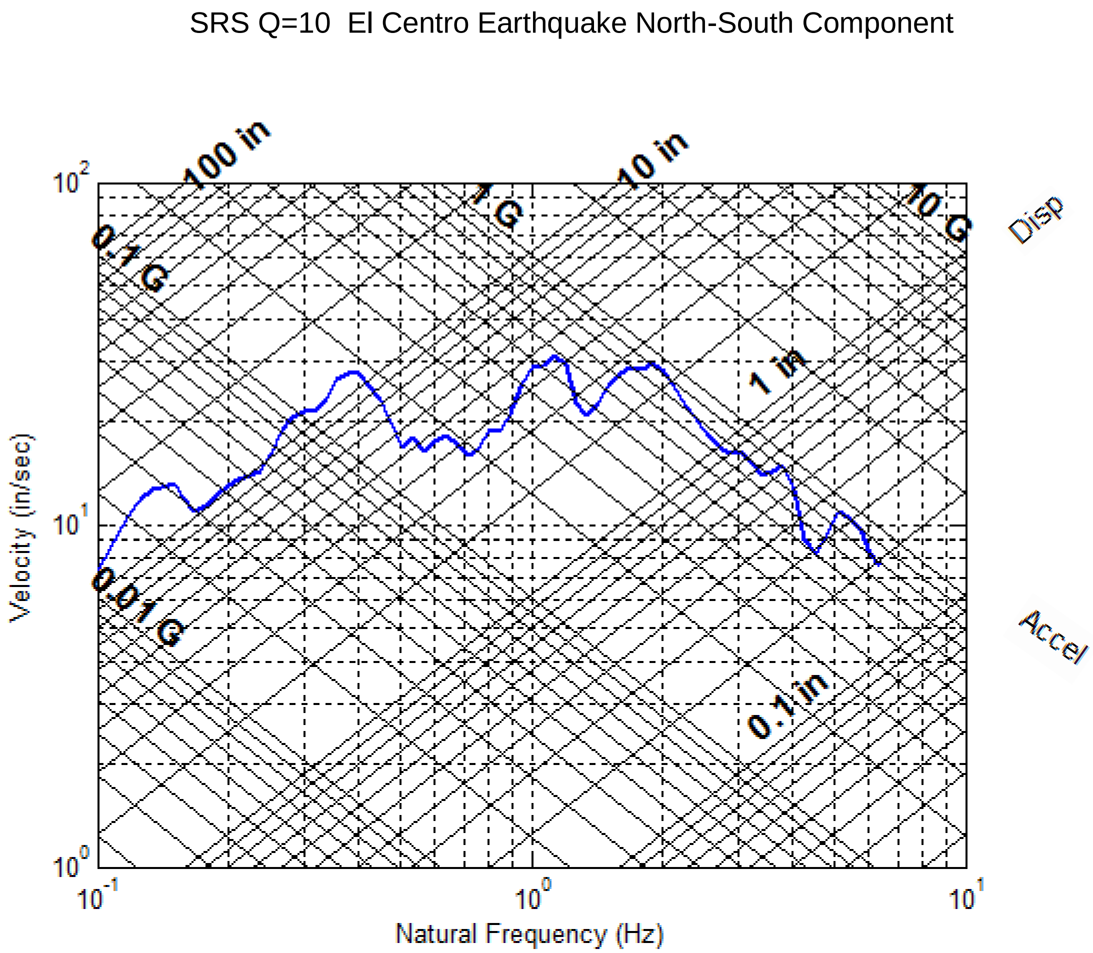

Figure L-2.

Table L-1. SRS, El Centro Earthquake, Results for the Domain from 0.1 to 6.4 Hz			
Parameter	Max	Min	Range (dB)
Displacement (inch)	15.0	0.2	38
Velocity (in/sec)	31.0	7.4	12
Acceleration (G)	0.93	0.012	38

The SRS of the time history is shown in Figure L-2 in tripartite format.

One of the advantages of the pseudo velocity SRS is that it has a smaller amplitude range than either the displacement or acceleration. The pseudo velocity SRS is thus less frequency-dependent.

APPENDIX M

Re-entry Vehicle Separation Shock

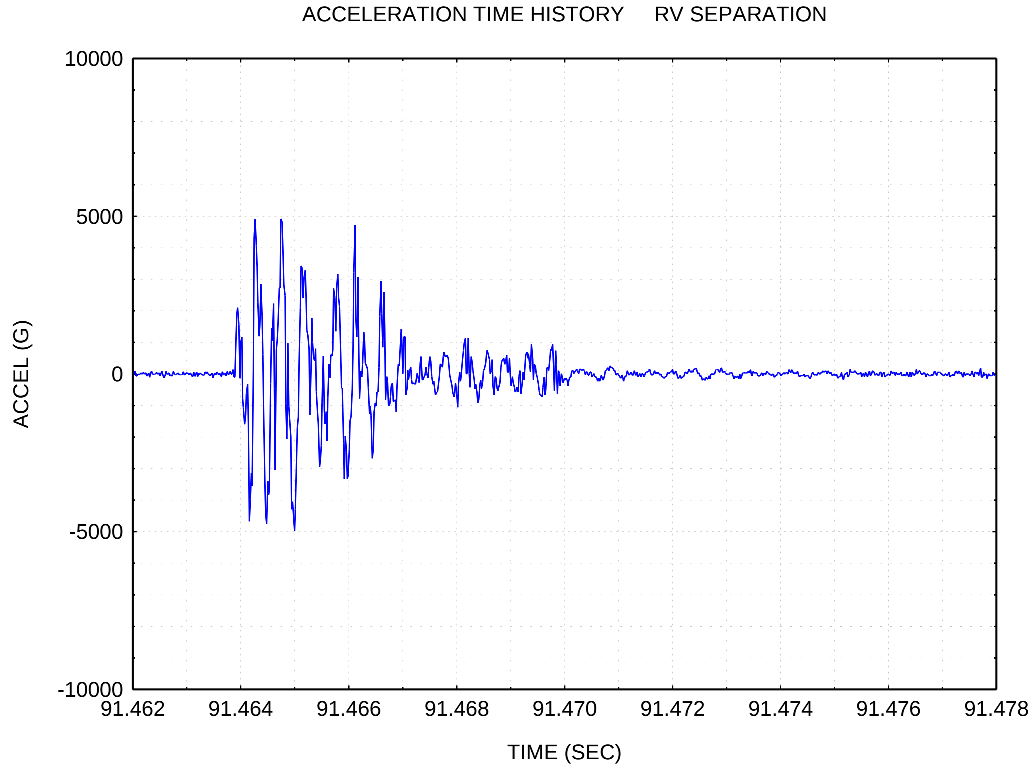

Figure M-1.

The time history is a near-field, pyrotechnic shock measured in-flight on an unnamed rocket vehicle. The separation device was linear shape charge.

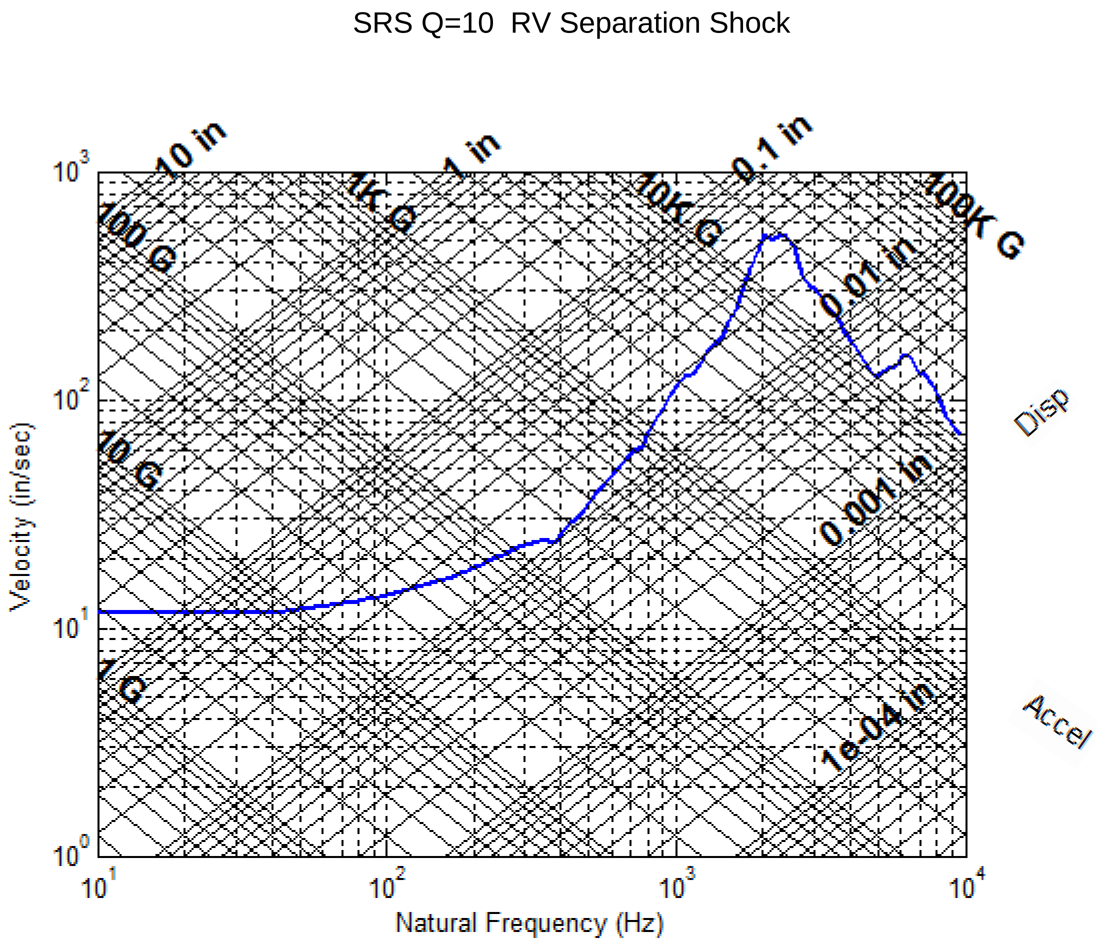

Figure M-2.

Table M-1. SRS, RV Separation, Results for the Domain from 100 to 10,000 Hz			
Parameter	Max	Min	Range (dB)
Displacement (inch)	0.041	0.0012	31
Velocity (in/sec)	526	14	31
Acceleration (G)	20,400	23	59

The SRS of the time history is shown in Figure M-2 in tripartite format.

The values in Table M-1 begin at 100 Hz because there is some uncertainty regarding the accuracy of the data below 100 Hz, which is typically the case for near-field pyrotechnic shock events. The velocity range is 28 dB lower than the acceleration range.

APPENDIX N

SR-19 Motor Ignition & Pressure Oscillation

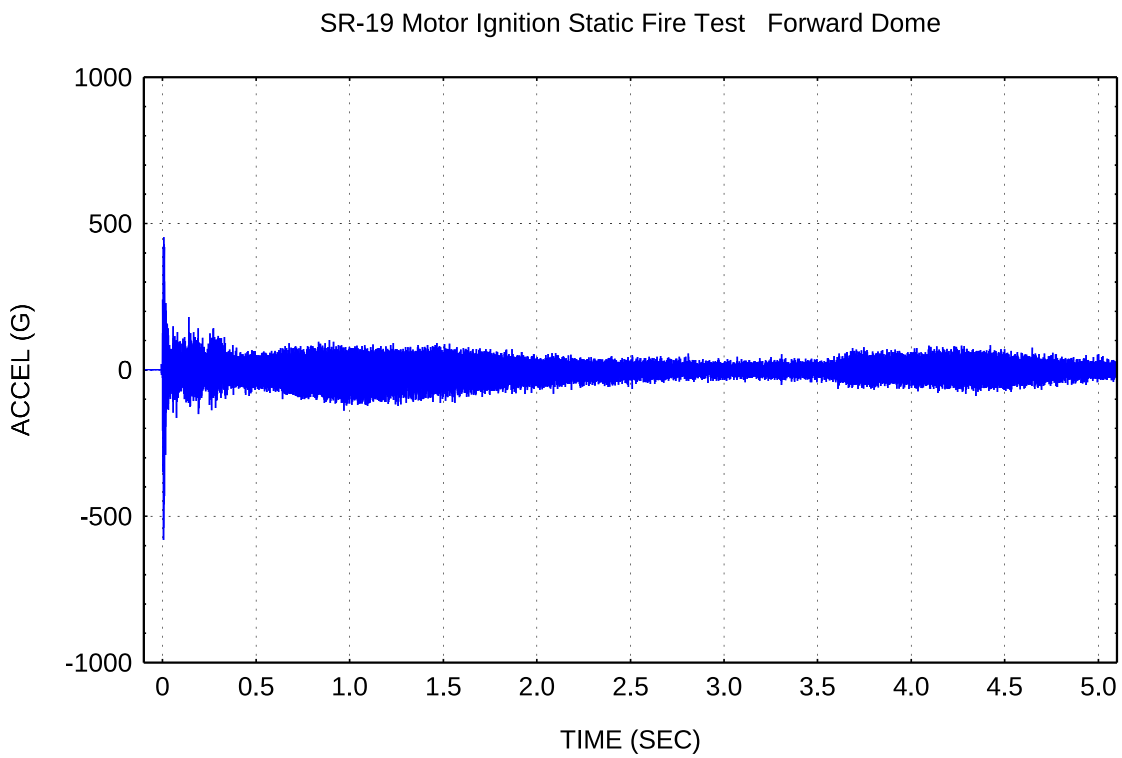

Figure N-1.

The SR-19 is a solid-fuel rocket motor. The combustion cavity has a pressure oscillation at 650 Hz.

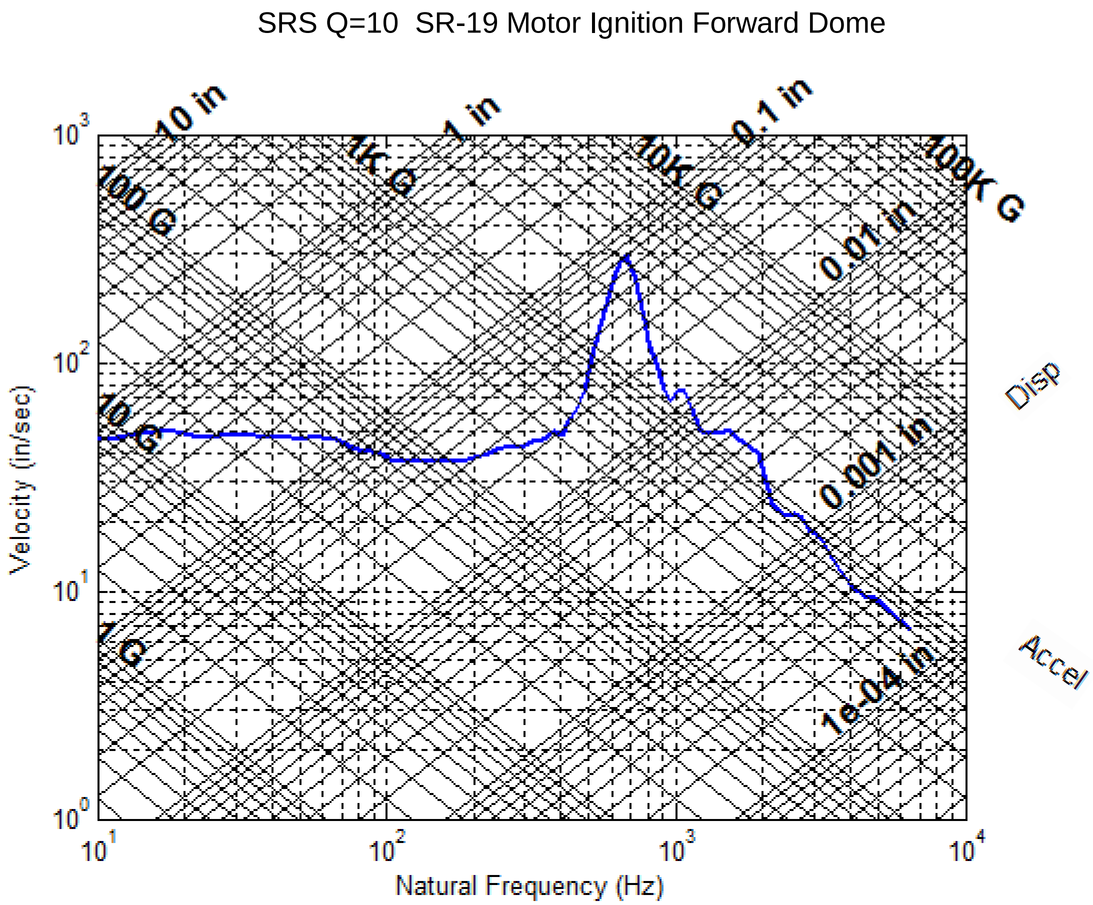

Figure N-2.

Table N-1. SRS, SR-19 Motor Ignition, Forward Dome, Results for the Domain from 10 to 6500 Hz			
Parameter	Max	Min	Range (dB)
Displacement (inch)	0.73	1.7e-04	73
Velocity (in/sec)	295	6.8	33
Acceleration (G)	3224	7.1	53

The peak at 680 Hz is due to the SR-19 motor oscillation which results from a standing pressure wave in the combustion cavity.

APPENDIX O

<u>Space Shuttle Solid Rocket Booster Water Impact</u>

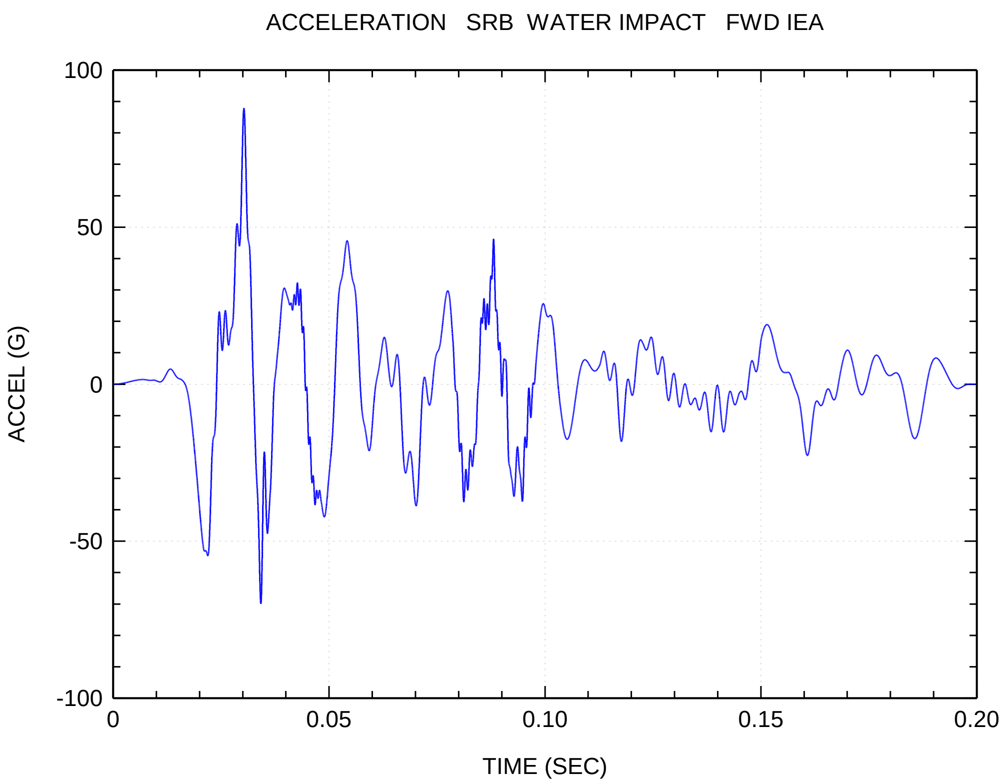

Figure O-1.

The data is from the STS-6 mission. Some high-frequency noise was filtered from the data.

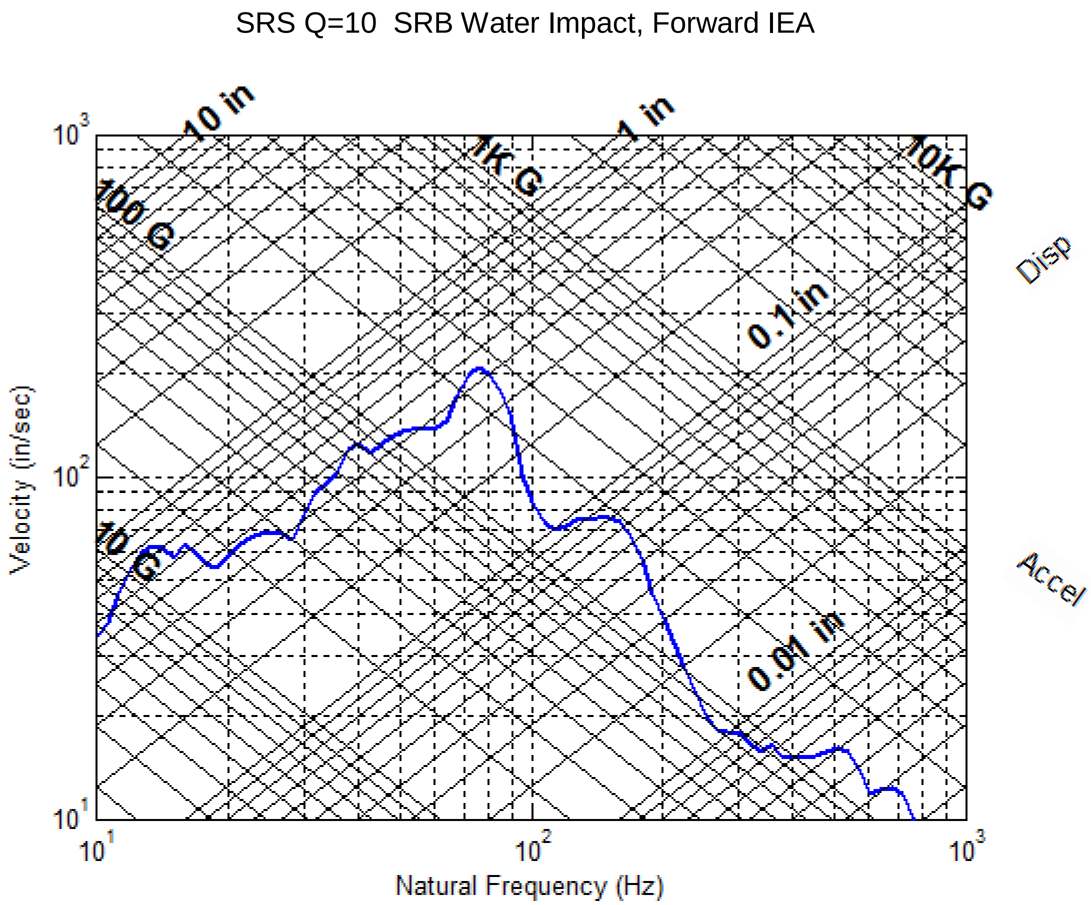

Figure O-2.

Table O-1. SRS, SRB Water Impact, Forward IEA, Results for the Domain from 10 to 750 Hz			
Parameter	Max	Min	Range (dB)
Displacement (inch)	0.76	0.002	52
Velocity (in/sec)	209	10	26
Acceleration (G)	259	5.6	33

The velocity SRS has the smallest dynamic range in terms of decibels.

APPENDIX P

V-band/Bolt-Cutter Shock

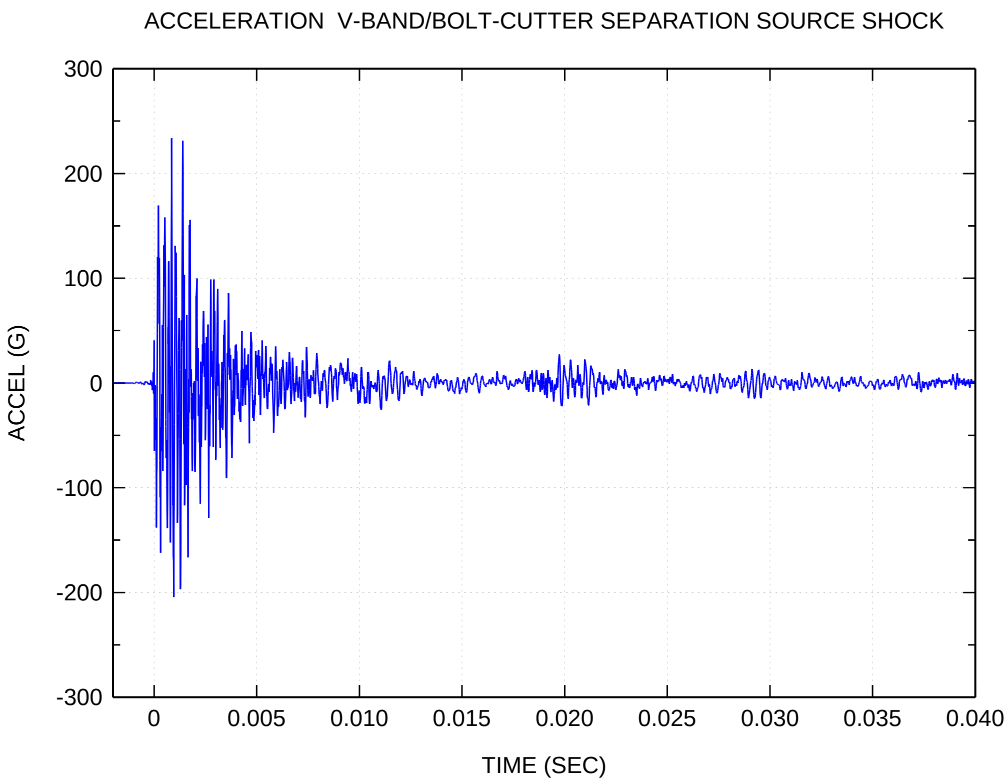

Figure P-1.

The time history was measured during a shroud separation test for a suborbital launch vehicle.

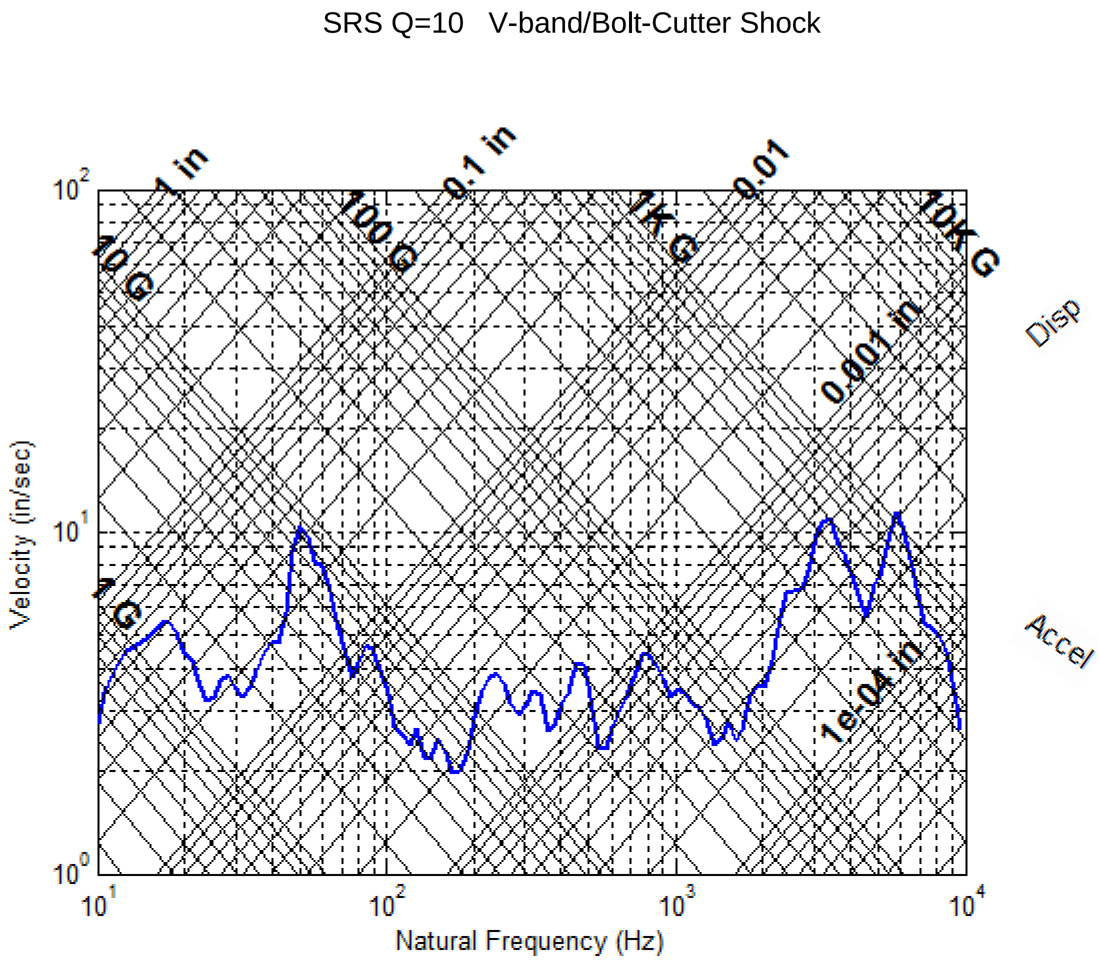

Figure P-2.

Table P-1. SRS Q=10, V-band/Bolt-Cutter Shock			
Parameter	Max	Min	Range (dB)
Displacement (inch)	0.032	4e-04	38
Velocity (in/sec)	11.4	2.0	15
Acceleration (G)	1069	0.4	69

The velocity SRS has the smallest dynamic range in terms of decibels.

APPENDIX Q

Maximum Velocity Summary

Table Q-1. Maximum Velocity & Dynamic Range of Shock Events		
Event	Maximum Pseudo Velocity (in/sec)	Velocity Dynamic Range (dB)
RV Separation, Linear Shape Charge	526	31
SR-19 Motor Ignition, Forward Dome	295	33
SRB Water Impact, Forward IEA	209	26
Half-Sine Pulse, 50 G, 11 msec	125	32
El Centro Earthquake, North-South Component	31	12
Half-Sine Pulse, 10 G, 11 msec	25	32
V-band/Bolt-Cutter Source Shock	11	15

The peak velocity comparison is useful, but a consideration of natural frequency is still needed because the dynamic range is greater than zero, at least 12 dB, in each case.

APPENDIX R

Velocity Limits of Materials

Gaberson gave the following limits in Reference 4.

Table R-1. Severe Velocities, Fundamental Limits to Modal Velocities in Structures						
Material	E (psi)	σ (psi)	ρ (lbm/in^3)	Rod V_{max} (in/sec)	Beam V_{max} (in/sec)	Plate V_{max} (in/sec)
Douglas Fir	1.92e+06	6450	0.021	633	366	316
Aluminum 6061-T6	10.0e+06	35,000	0.098	695	402	347
Magnesium AZ80A-T5	6.5e+06	38,000	0.065	1015	586	507
Structural Steel, High Strength	29e+06	33,000 100,000	0.283	226 685	130 394	113 342

The following tables are taken from Reference 29. The original sources are noted. The velocity terms are "modal velocities at the elastic limit."

(*Values from Sloan, 1985, Packaging Electronics*)

Material	E (1e+06 psi)	μ	ρ (lbm/in^3)	σ_{ult} (ksi)	σ_{yield} (ksi)	v_{rod} (in/sec)	v_{beam} (sec)
Aluminum 5052	9.954	0.334	0.098	34	24	477.4	275.9
Aluminum 6061-T6	9.954	0.34	0.098	42	36	716.2	413.9
Aluminum 7075-T6	9.954	0.334	0.1	77	66	1299.8	751.3
Be	42	0.1	0.066	86	58	684.5	395.7
Be-Cu	18.5	0.27	0.297	160	120	1005.9	581.5
Cadmium	9.9	0.3	0.312	11.9	11.9	133.0	76.9
Copper	17.2	0.326	0.322	40	30	250.5	144.8
Gold	11.1	0.41	0.698	29.8	29.8	210.4	121.6
Kovar	19.5	-	0.32	34.4	59.5	468.0	270.5
Magnesium	6.5	0.35	0.065	39.8	28	846.4	489.3
Nickel	29.8	0.3	0.32	71.1	50	318.1	183.9
Silver	10.6	0.37	0.38	41.2	41.2	403.4	233.2
Solder 63/37	2.5	0.4	0.30008	7	7	158.8	91.8
Steel 1010	30	0.292	0.29	70	36	239.8	138.6
Stainless	28.4	0.305	0.29	80	40	273.9	158.3
Alumina al203	54	-	0.13	25	20	148.3	85.7
Beryllia Beo	46	-	0.105	20	20	178.8	103.4
Mira	10	-	0.105	-	5.5	105.5	60.0
Quartz	10.4	0.17	0.094	27.9	27.9	554.5	320.5
Magnesia Mgo	10	-	0.101	12	12	234.6	135.6
EPO GLS G10 X/Y	2.36	0.12	0.071	25	35	1680.1	971.1
EPO GLS G10 Z	2.36	0.12	0.071	25	35	1680.1	971.1
Lexan	0.379	-	0.047	9.7	9.7	1428.1	825.5
Nylon	0.217	-	0.041	11.8	11.5	2395.6	1384.8
Teflon	0.15	-	0.077	-	4	731.3	422.7
Mylar	0.55	-	0.05	25	25	2962.2	1712.3

(*Values from Roark, 1965, p 416*)

Material	E (1e+06 psi)	μ	ρ (lbm/in^3)	σ_{ult} (ksi)	σ_{yield} (ksi)	v_{rod} (in/sec)	v_{beam} (sec)
Aluminum Cast Pure	9	0.36	0.0976	11	11	230.6	133.3
Al Cast 220-T4	9.5	0.33	0.093	42	22	459.9	265.8
Al 2014-T6	10.6	0.33	0.101	68	60	1139.4	658.6
Beryllium Cu	19	0.3	0.297	150	140	1158.0	669.4
Cast Iron, Gray	14	0.25	0.251	20	37	357.8	224.2
Mg AZ80A-T5	6.5	0.305	0.065	55	38	1148.7	663.0
Titanium Alloy	17	0.33	0.161	115	110	1306.5	755.2
Steel Shapes	29	0.27	0.283	70	33	226.3	130.8
Concrete	3.5	0.15	0.0868	0.35	0.515	18.4	10.6
Granite	7	0.28	0.0972	-	2.5	59.6	34.4

APPENDIX S

Characteristic Impedance Values

Note that: 1 Pa sec/m = 1 kg/(m^2 sec)

Material	Density (kg/m^3)	Elastic Modulus (GPa)	Speed (m/sec)		Characteristic Impedance (MPa sec/m)	
			Bar	Bulk	Bar	Bulk
Aluminum	2700	71	5150	6300	13.9	17.0
Steel	7700	195	5050	6100	39.0	47.0

Material	Density (lbm/in^3)	Elastic Modulus (psi)	Speed (in/sec)		Characteristic Impedance [lbm/(in^2 sec)]	
			Bar	Bulk	Bar	Bulk
Aluminum	0.1	1e+07	2.03e+05	2.48e+05	2.03E+04	2.48E+04
Steel	0.285	3e+07	1.99e+05	2.40e+05	5.67E+04	6.84E+04

Material	Characteristic Impedance (psi sec/in)	
	Bar	Bulk
Aluminum	52.5	64.2
Steel	147	173

APPENDIX T

Velocity Limits for Buildings

Recommended limit values for traffic are given in Table T-1, as taken from References 22 through 24. The peak value is taken from the velocity time history.

Table T-1. Recommended Ground Limit Values for Traffic

Type of building and foundation	Recommended Vertical Velocity Vmax	
	(mm/sec)	(in/sec)
Especially sensitive buildings and buildings of cultural and historic value	1	0.039
Newly-built buildings and/or foundations of a foot plate (spread footings)	2	0.079
Buildings on cohesion piles	3	0.12
Buildings on bearing piles or friction piles	5	0.20

The vertical velocity is with respect to the ground vibration.

The specification implies that building stress correlates more closely with velocity than with either displacement or acceleration.

APPENDIX U

This appendix is not concerned with vibration stress per se. It is included to show how velocity is the amplitude metric of choice in industries outside of aerospace.

Velocity Limits for Vibration Sensitive Equipment

Colin Gordon, Reference 25, has derived generic criterion curves, with an emphasis on semiconductor facilities, as shown in Table U-1 and in Figure U-1. The velocity is measured in one-third octave bands over the frequency range from 8 Hz to 100 Hz. The limits are for floor measurements.

Table U-1. Generic Vibration Criterion Curves			
Criterion Curve	Max Level Velocity RMS (micrometers/sec)	Detail Size (microns)	Description of Use
Workshop (ISO)	800	N/A	Distinctly feelable vibration. Appropriate to workshops and nonsensitive areas.
Office (ISO)	400	N/A	Feelable vibration. Appropriate to offices and nonsensitive areas.
Residential Day (ISO)	200	75	Barely feelable vibration. Appropriate to sleep areas in most instances. Probably adequate for computer equipment, probe test equipment and low-power (to 20X) microscopes.
Theater (ISO)	100	25	Vibration not feelable. Suitable for sensitive sleep areas. Suitable in most instances for microscopes to 100X and for other equipment of low sensitivity.
VC-A	50	8	Adequate in most instances for optical microscopes to 400X, microbalances, optical balances, proximity and projection aligners, etc.
VC-B	25	3	An appropriate standard for optical microscopes to 1000X, inspection and lithography equipment (including steppers) to 3 micron line widths.
VC-C	12.5	1	A good standard for most lithography and inspection equipment to 1 micron detail size.
VC-D	6	0.3	Suitable in most instances for the most demanding equipment including electron microscopes (TEMs and SEMs) and E-Beam systems, operating to the limits of their capability.
VC-E	3	0.1	A difficult criterion to achieve in most instances. Assumed to be adequate for the most demanding of sensitive systems including long path, laser-based, small target systems and other systems requiring extraordinary dynamic stability.

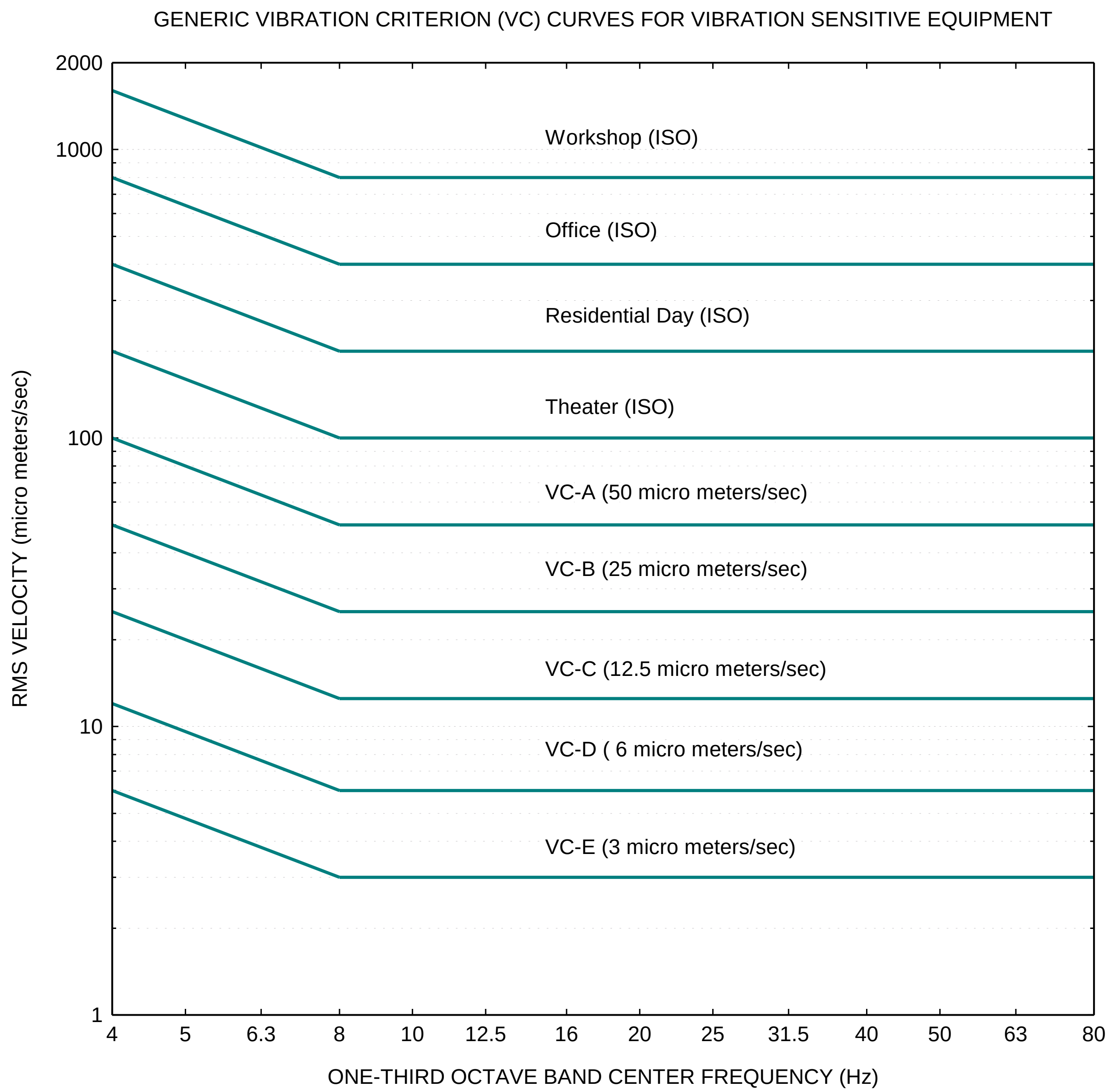
GENERIC VIBRATION CRITERION (VC) CURVES FOR VIBRATION SENSITIVE EQUIPMENT
RMS VELOCITY (micro meters/sec)
2000
1000
100
10
1
Workshop (ISO)
Office (ISO)
Residential Day (ISO)
Theater (ISO)
VC-A (50 micro meters/sec)
VC-B (25 micro meters/sec)
VC-C (12.5 micro meters/sec)
VC-D (6 micro meters/sec)
VC-E (3 micro meters/sec)
4
5
6.3
8
10
12.5
16
20
25
31.5
40
50
63
80
ONE-THIRD OCTAVE BAND CENTER FREQUENCY (Hz)

Figure U-1.